

Review

Elucidating the mechanisms of Paraffin-Olefin separations using nanoporous adsorbents: An overview

Dipendu Saha,^{1,*} Min-Bum Kim,² Alexander J. Robinson,² Ravichandar Babarao,^{3,4} and Praveen K. Thallapally²

SUMMARY

Light olefins are the precursors of all modern-day plastics. Olefin is always mixed with paraffins in the time of production, and therefore it needs to be separated from paraffins to produce polymer-grade olefin. The state-of-the-art separation technique, cryogenic distillation, is highly expensive and hazardous. Adsorption could be a novel, sustainable, and inexpensive separation strategy, provided a suitable adsorbent can be designed. There are different types of mechanisms that were harnessed for the separation of olefins by adsorption, and in this review, we have focused our discussion on those mechanisms. These mechanisms include, (a) Affinity-based separation, like pi complexation and hydrogen bonding, (b) Separation based on pore size and shape, like size-exclusion and gate-opening effect, and (c) Non-equilibrium separation, like kinetic separation. In this review, we have elaborated each of the separation strategies from the fundamental level and explained their roles in the separation processes of different types of paraffins and olefins.

INTRODUCTION: NEED AND TYPES OF SEPARATION

Separation of olefins and paraffins is one of the key seven separation needs of the modern world (Sholl and Lively, 2016). The main type of olefin and paraffin separation is attributed to the purification and isolation of ethylene from ethane and propylene from propane. Ethylene and propylene are the precursors or monomers of two most important polymeric plastics of modern society, polyethylene and polypropylene. Owing to the high global demand in plastic production, light olefins have reached an enormous worldwide production of 200 million tons with the market value of \$ 254.6 billion in 2016. It is expected to reach \$ 475.8 billion by 2023 (<https://www.marketresearchfuture.com/reports/light-olefin-market-1037> (Accessed June 2018)). The global production of olefins can be approximated as 30 kgs of olefin per person on earth. In the last decade, the olefin production has increased over 50% owing to the demand from developing countries (Sholl and Lively, 2016). The key technique to produce C2 and C3 olefins is the steam cracking of naphtha and C2/C3 paraffins and owing to the thermodynamic constraints, the conversion is not more than 20–40% (Moulijn et al., 2001). In the pool of product mixtures, the key separation needed lies with the separation of C2/C3 olefins from their corresponding paraffins. The purity of polymer grade olefin must be more than 99.95%.

Although the separation of ethylene and propylene are the key separation needs in the class of olefin separation, there are few other types of olefin separation that are also important in the chemical industry.

- (a) *Separation of ethylene from acetylene*: During the production of ethylene by cracking of ethane, a few other hydrocarbons are also generated, including acetylene, usually in the range of 1%. Presence of acetylene in ethylene as the monomer of polymerization is undesirable because, (i) it can poison the polymerization catalyst (Hu et al., 2015) and (ii) it can form solid metal acetylides that may block the fluid stream causing explosion in pipelines (Molero et al., 1999).
- (b) *Separation of propylene from propyne*: In the course of production of propylene by steam cracking of hydrocarbons or petroleum distillate, along with other byproducts, a small amount propyne (C₃H₄) is also produced. The concentration of propyne is in the range of 1,000–2,000 ppm (Yang et al., 2018a, 2018b). In order to obtain the polymer grade propylene, the concentration of propyne in the feed mixture must be less than 5 ppm. Separation of propyne from propylene is extremely difficult because of two reasons, (i) similar molecular size of propylene and propyne

¹Chemical Engineering Department, Widener University, 1 University Place, Chester, PA 19013, USA

²Pacific Northwest National Laboratory, Richland, WA 99352, USA

³Applied Chemistry and Environmental Science, School of Science, RMIT University, Melbourne, Australia

⁴CSIRO Manufacturing Flagship, Clayton, VIC, Australia

*Correspondence: dsaha@widener.edu
<https://doi.org/10.1016/j.isci.2021.103042>



(propylene: $5.25 \times 4.16 \times 6.44 \text{ \AA}^3$; propyne: $4.16 \times 4.01 \times 6.51 \text{ \AA}^3$), and (ii) very low concentration of propyne in the mixture.

- (c) *Separation of ethylene from the product mixtures of oxidative coupling of methane (OCM)*: Unlike conventional methods, synthesis of ethylene from oxidative coupling of methane (OCM) is considered as more sustainable owing to the high availability of methane as shell gas and its clean nature. However, the yield of ethylene in OCM is very small and there are several by-products. In OCM, ethylene needs to be separated (Zhang et al., 2021; Bachman et al., 2018) from C_2H_6 , CH_4 , CO_2 , CO and H_2 .
- (d) *Separation of Styrene from ethylbenzene*: Styrene is an essential monomer that is employed to produce varieties of polymeric products, including synthetic rubbers, resins and different thermoplastics. Styrene is produced by the partial dehydrogenation of ethylbenzene. Because of the thermodynamic constraints, 20–40% ethylbenzene remains in the product stream and it needs to be removed in order to achieve a polymer-grade styrene.
- (e) *Separation of Propylene from nitrogen*: After completion of polymerization of propylene to polypropylene, the product mixture contains unreacted propylene and it is usually purged by nitrogen gas. Typically, the purge mixture contains 70% N_2 and 30% propylene (Ribeiro et al., 2013; Han et al., 2005; Tan et al., 2019). As of today's scenario, no industrial method is economically viable to separate propylene and hence it is not recovered from the purge mixture. It is sent to a flare stack for burning in air. It is estimated that around 2,000–4,000 tons of propylene is wasted in this process that counts for around \$ 1.5 million per year for the entire purge mixture including nitrogen (Ribeiro et al., 2013).
- (f) *Separation of 1,3-butadiene from C4 hydrocarbons*: 1,3-butadiene is the precursor of synthetic rubber. It is generally obtained from the C4 hydrocarbon mixtures containing 1 and 2-butene, isobutene, isobutane and *n*-butane, where composition of 1,3-butadiene is around 39.5% (Schulze and Homann, 1989). To obtain polymer-grade 1,3-butadiene, it needs to be separated from the rest of C4 hydrocarbons.

CURRENT AND STATE-OF-THE ART SEPARATION AND ITS DRAWBACKS

Owing to the very close physiochemical properties of light olefins, such as boiling points, with their corresponding paraffins, it is very difficult to separate them. Figure 1 shows the molecular size, kinetic diameters and polarizability of different hydrocarbons.

Fractional distillation is the most commonly used separation technology in the process industries for recovery of valuable alkenes, such as ethylene and propylene, from mixtures with the corresponding saturated alkanes. The boiling points are all below ambient temperature, and therefore the distillation separations must be carried out under cryogenic conditions. Therefore, the current state-of-the-art separation process of ethylene from ethane and propylene from propane involves cryogenic distillation that harnesses a small difference in boiling points between ethylene/ethane and propylene/propane in the cryogenic range. To obtain a high quality and polymer grade olefins, the distillation must be operated at the extreme conditions of temperature and pressure. For cryogenic separation of ethane and ethylene, the distillation column must be maintained at the temperature and pressure of -25°C and 23 bars, respectively, whereas, for the propane/propylene separation, the distillation column should be maintained at the conditions of -30°C and 3 bar (Saha et al., 2020). The cryogenic distillation column also needs to be very tall, consisting of about 120–180 trays and operating at high reflux ratio. The energy consumption of distillation separations arises from the need for phase changes in condensers/reboilers; the energy consumption increases with increasing reflux ratio (required when the relative volatilities are low, as for alkene/alkane mixtures) and when operating temperature is below ambient. Such a design requires a high energy input (Saha et al., 2020) of 7GJt^{-1} . The capital cost of installing cryogenic separation unit of ethylene is around twenty million dollars with the utility costs more than one million dollar every year (<http://separationtechnology.com/separation-of-ethylene-from-ethane/> (accessed July 2021)). The operation of a cryogenic distillation unit is highly energy intensive. It utilizes about 0.12 quads ($1 \text{ Quad} = 10^{15} \text{ BTU}$) of energy annually in 1991 (Saha et al., 2020), which is equivalent to 0.3% of global energy usage and accounts for the annual energy consumption of a small country, like Singapore. In addition, the whole process of a cryogenic distillation is hazardous owing to the exposure of cryogenic temperature.

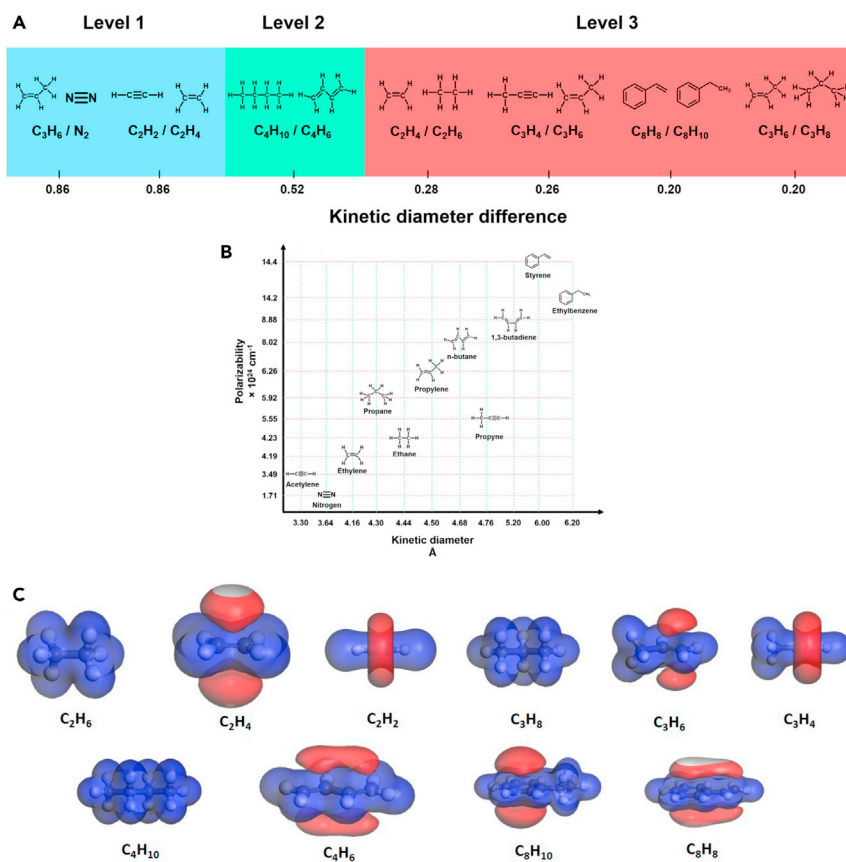


Figure 1. Different properties of hydrocarbon molecules

(A) Complex hydrocarbons separation levels according to molecular size difference.
(B) The hydrocarbons classified by the kinetic diameter and polarizability.
(C) Molecular sizes, kinetic diameter and electrostatic potential for different hydrocarbons.

There are few other separation strategies that are also involved in the separation of different other types of olefins as mentioned in the later parts of the introduction. In the petrochemical industry, the state-of-the-art separation technique to isolate ethylene from acetylene includes partial hydrogenation of acetylene to ethylene by supported Pd catalyst and solvent extraction of cracked olefin by organic solvents, like DMF or acetone 90 (Hu et al., 2015). The process of dehydrogenation suffers from the need of expensive catalysts and loss of ethylene because of excessive hydrogenation, whereas the solvent extraction leaves hazardous and costly solvents as wastes. In order to separate propylene from propyne in an industrial scale, propyne is usually hydrogenated by noble metals (Ribeiro et al., 2013). The process of hydrogenation is highly energy intensive and did not improve in 50 years. Owing to the small difference in boiling points of styrene (418 K) and ethylbenzene (409 K), vacuum and extractive distillation processes were employed to separate them in an industrial scale and in presence of some polymerization inhibitors, like phenylene diamines or dinitrophenols. Extractive distillation is also employed to separate 1,3 butadiene from the rest of the C4 hydrocarbon mixtures. In this extraction distillation, three types of solvents are usually employed, acetonitrile (ACN), dimethylformamide (DMF) and N-methyl pyrrolidone (NMP). All the extractive distillation processes are quite expensive and often leave undesirable and hazardous residues of solvents (Gehre et al., 2017; Schulze and Homann, 1989).

SEPARATION OF OLEFINS AND PARAFFINS BY ADSORPTION

Unlike traditional processes, like cryogenic distillation, adsorption is a benign, inexpensive and sustainable process (Saha and Grappe, 2017; Yang, 1987; Do, 1998). In adsorption, one of the components of paraffin or olefin is preferentially adsorbed in the suitably designed pores of the adsorbent leaving behind the other.

Therefore, the key challenge of employing adsorption in the separation of paraffin and olefin is designing and synthesizing the suitable adsorbent that can selectively or preferentially adsorb the olefin or paraffin component of the mixture. Despite an extremely large number of adsorbents having been synthesized with time, only a small fraction of them was proven to be successful in performing the separation. Traditionally, surface modified zeolite, silica or alumina demonstrated the possible separation.

With time, metal-Organic Frameworks (MOFs), covalent organic frameworks (COFs), and hydrogen-bonded organic frameworks (HOFs) have been introduced with excellent separation characteristics and several structures of porous materials were reported with superior performance compared to that of traditional adsorbents. MOFs (Lin et al., 2019) are crystalline porous materials where metal nodes are connected with organic linkers via coordination bonds. On the other hand, COFs are crystalline microporous materials that self-assemble into two/three-dimensional (2D/3D) network structures with uniform pore sizes linked by strong covalent bonds as opposed to metal coordination bonds found in MOFs. Given the strong covalent bond between the molecular building units used in COF synthesis, they have exceptional stability in acidic and basic media similar to some MOFs. Typically, COFs can be synthesized based on the type of functional groups used on the molecular building unit. For example, condensation of boronic acid on a molecular building unit converges to form 2D or 3D COF based on boronate linkages. Therefore over the past decade, COFs with boroxine, boronate, imine, hydrazine, azine, imide, -P-O-, -C=C-, -C-NH-, 1,4-dioxin linkages have been synthesized using the appropriate functional groups and various types of molecular building units. HOFs are self-assembled porous structures stabilized by intermolecular hydrogen-bonding interaction. Significant progress has been made in design and development of HOFs for gas storage and separation applications. Large number of HOFs are solution processable as opposed to MOFs and COFs makes them unique.

Recently, surface engineered nanoporous carbons also demonstrated good separation characteristics. Different types of mechanisms that were employed to separate the mixtures are pi complexation, hydrogen bonding, size exclusion or kinetic separation and these mechanisms are further elaborated in detail in the later sections. In this regard, the readers should be aware that a lab-scale demonstration of a successful separation of paraffins and olefins by an adsorbent may not always indicate that it can be successfully employed in a large scale. Different other factors, including long-term stability, sensitivity to the other environmental conditions, like moisture and cost (economy) of the adsorbent and adsorption processes also play a crucial role in selecting the adsorbent, which are beyond the scope of this review.

Different adsorption processes that can be employed for gas separation are pressure swing adsorption (PSA) (Ruthven, 1984; Saha et al., 2016) and temperature swing adsorption (TSA). In PSA, pressure is varied to adsorb and desorb the preferred component, whereas temperature is varied for TSA. Being a far more common process in industry, PSA employs multiple fixed bed adsorption columns for continuous adsorption and regeneration purposes. For two-component (binary) adsorption, the common metric that is used to study the preferential adsorption of one component over another is referred to as selectivity (α_{1-2}) and defined as

$$\alpha_{1-2} = \frac{x_1/y_1}{x_2/y_2} \quad (\text{Equation 1})$$

where component "1" is the preferred component over "2". x and y are the mole fractions of adsorbed phase and bulk phase, respectively. As the experiment on mixed gas adsorption is extremely cumbersome owing to the complex experimental requirements, Ideal Adsorbed Solution Theory (IAST) has become very popular among researchers to calculate the selectivity from pure component gas adsorption isotherms (Myers and Prausnitz, 1965).

Adsorbent selection parameter (S), is also often used in pressure swing adsorption (PSA) and defined as (Saha et al., 2010)

$$S = \frac{\Delta q_1}{\Delta q_2} S_{ads} \quad (\text{Equation 2})$$

where Δq_1 and Δq_2 are the working capacity of two components, '1' and '2', respectively. Quite often, the adsorbent selection parameter becomes more useful as it incorporates the working capacity of the individual gases.

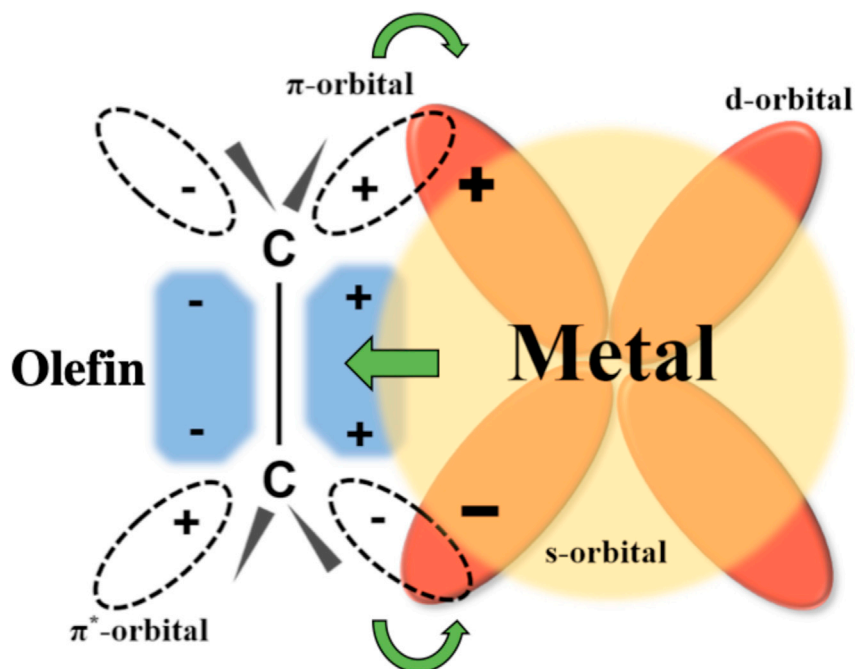


Figure 2. Schematic representation of π -complexation

MECHANISMS OF SEPARATION

Adsorptive separation consists of three key mechanisms, (a) Affinity-based separation, (b) Separation based on pore size and shape, and (c) Kinetic separation. In the course of three basic separation techniques of adsorption, the readers should be aware that sometimes multiple separation mechanisms have been harnessed to achieve some particular separation (Chen et al., 2019).

Because of the very similar physical and chemical properties of olefins/paraffins, it is very difficult to separate these molecules from one another. The kinetic diameters of ethane, ethylene, propane and propylene are very close (ethane: 4.443 Å; ethylene: 4.163 Å; propane: 4.3–5.118 Å and propylene: 4.678 Å) (Saha et al., 2020). However, sorbents with precise control over pore size/shape (kinetic separation or size exclusion or also known as beyond equilibrium) and topology can play a significant role in separating closely related molecules (Li et al., 2018). Apart from these geometrical factors, interactions between host and guest (hydrogen bonding) that include electrostatics, π -complexation, weak, strong intermolecular directional and non-directional interactions can also play a crucial role (Equilibrium or thermodynamic separation). Figure 1 shows the molecular size of different paraffins and olefins (a) their kinetic diameter and polarizability (b) and Isosurface maps of the electrostatic potential (EP) for different hydrocarbons (c).

Affinity-based separation

π complexation

The π -complexation method is the most common and widely used affinity-based separation in the field of olefin purification. The presence of π -electron cloud and higher quadrupole moment, olefins tend to form π -complexation with few specific metals as opposed to paraffins. It has been presented that π -complexation can be demonstrated by d-block transition metals of the periodic table, from Sc to Cu, from Y to Ag and from La to Au of the periodic table. Ag(I) and Cu(I) were most successfully employed to implement π complexation, whereas Ag(I) was the most prevalent for this purpose. In the course of π -complexation, the outer d and s molecular orbitals in metals are known to form π bonds with electron rich guest molecules (Figure 2). The σ bond forms via the overlap of the π electron cloud in olefins with vacant outermost s-orbital of the metal and π bond forms via the metal back donation from d-orbital to the vacant π^* anti-bonding orbitals. The outer s molecular orbital in metal is also known to form π bonds with electron rich molecules. However, the π -complexation depends on various factors such as number of d- and π -electrons

in metal, olefins and the ability to donate to engage in bond formation. Different types of adsorbents, including alumina, silica, zeolite, carbon and MOFs demonstrated π -complexation upon surface or structure modification.

The first MOF explored for separation of olefin/paraffin was using CuBTC (BTC = 1,3,5-benzene-tricarboxylate), which possesses three different types of interconnected cavities; the first is located in the middle of the unit cell with pore limiting diameter (PLD) of 11 Å with exposed unsaturated open metal sites (OMSs) which is connected to slightly larger cage with 13 Å PLD, whereas the third is a small tetrahedral cavity with 5 Å PLD. The single-component adsorption of ethylene results in an excess of 6 mmol g⁻¹ at 298 K and 100 kPa pressure. The steep uptake of ethylene at low pressure was explained by the strong π -complexation between open metal sites with ethylene molecules. CuBTC with exposed Cu(II) sites was also employed for propylene and propane separation (Lamia et al., 2009). The X-ray diffraction experiments with CuBTC suggested that the propane molecule tends to bind in small octahedral pockets. The larger molecules such as butene are excluded owing to the larger size whereas propylene strongly binds with Cu(II) centers via π -complexation. The existence of such a strong interaction between π -orbitals of propylene and unsaturated metal sites in CuBTC resulted in selective separation of propylene from propane. This example provides an importance of OMS in separation of propylene from propane based thermodynamic equilibria and molecular sieving mechanism to separate out larger molecules such as butene (molecular sieving).

Like CuBTC, M₂(dobdc) (where dobdc = 2,5-dihydroxy-1,4-benzenedicarboxylic acid) (also known as MOF-74-M) are another class of MOFs with high density of OMS. Extensive experiments on MOF-74 series suggest the OMSs play a significant role in gas adsorption and separation. MOF-74-Mg contains 11 Å channels and the pore walls are aligned with square pyramidal M²⁺ centers with accessible OMS for incoming hydrocarbon molecules. To further improve the selectivity of C₂H₄/C₂H₆, a redox-active MOF-74 was synthesized with high density of Fe²⁺ sites as OMS (Bloch et al., 2012). The *in-situ* neutron diffraction experiments MOF-74-Fe with various olefins/paraffins showed structure property relationship between host and guest hydrocarbon molecules. Furthermore, *in-situ* experiments confirmed that the olefins molecules have interactions with MOF-74-Fe with shorter Fe–C bond distance (2.4 Å) compared to that of paraffins (3.0 Å), indicating stronger affinity toward olefins. This strong affinity for each gas was further verified by calculating the adsorption enthalpy (ethylene: –45 kJ mol⁻¹). The IAST-based selectivity of C₂H₄/C₂H₆ was in the range of 13–18 for an equimolar mixture at 318 K which is higher than zeolite NaX and isostructural MOF-74-Mg. The first-principle calculations suggest different types of binding mechanism may contribute to the elevated adsorption of olefins, including electrostatic force, van der Waal force, and charge transfer interactions between olefin and OMS. Furthermore, gas-gas interactions were also found to play a critical role in binding energies.

To further improve the binding efficiencies by OMS, a series of MOFs were synthesized of the type M₂(m-dobdc) (M = Mg, Mn, Fe, Co, Ni; m-dobdc = 4,6-dioxido-1,3-benzenedicarboxylate) by replacing the organic ligand found in MOF-74 with metal substituted H₄(m-dobdc) ligand (Bachman et al., 2017). Among all the M₂(m-dobdc) MOFs, Fe₂(m-dobdc) shows the highest C₂H₄/C₂H₆ selectivity of 25 and C₃H₆/C₃H₈ selectivity of 55 at 298 K and 1 bar. The *in-situ* X-ray diffraction experiments reveal the improvement in selectivity arising from increased charge density at the metal sites. Fe₂(m-dobdc) and Mn₂(m-dobdc) were also demonstrated as ethylene selective adsorbents for its separation from C₂H₆, CH₄, CO₂, CO and H₂ in the OCM reaction (Bachman et al., 2018)

Selective adsorption of propylene over propane was reported in MOF-74-M (M = Mg, Co and Mn). Among three MOFs tested, MOF-74-Co was proven to have exceptional propylene/propane selectivity of 46 suggesting strong π -complexation between propylene and Co(II) sites. The results of a Grand Canonical Monte Carlo (GCMC) simulation on MOF-74 (Mg and Co) (Bae et al., 2012) confirmed that MOF-74 series are olefin selective because of its strong interaction between the OMSs and olefin molecule through π -complexation. GCMC simulations indicated propylene has a stronger affinity towards MOF-74 over ethylene because of the significant difference in dipole moment.

Apart from MOFs containing OMSs, an Ag(I) doped porous aromatic frameworks (PAFs) was also reported, named as PAF-1-SO₃Ag (Li et al., 2014). After ion exchange, these compounds were used for adsorptive separation of ethylene from ethane. The ethylene/ethane separation selectivity of PAF-1-SO₃Ag was

reported to be 27, which is very high compared to conventional adsorbents including many other MOFs. The Ag(I) was stably incorporated to PAF-1-SO₃Ag that exhibits a higher adsorption enthalpy of -106 kJ mol^{-1} compared to PAF-1 (-14 kJ mol^{-1}) and PAF-1-SO₃H (-23 kJ mol^{-1}) because of the strong π -complexation interaction between Ag(I) and the ethene molecules. The heat of adsorption of ethylene on PAF-1-SO₃Ag was significantly higher than the adsorption enthalpy of MOFs with OMS, signifying that MOFs containing π -electron rich metal ions is more advantageous for ethylene adsorption than MOFs with OMSs. Similarly, olefin selective properties also appear in MIL-101(Cr)-SO₃Ag that can be attributed to the presence of Ag(I) (Zhang et al., 2015). The MIL-101(Cr)-SO₃Ag showed a higher olefin selectivity than conventional adsorbents due to the strong interaction by π -complexation between Ag(I) ion and olefin molecules. The *in-situ* Infrared experiments with ethylene in PAF-1-SO₃Ag and MIL-101-SO₃Ag suggest strong infrared spectroscopy (IR) features at $970\text{--}980 \text{ cm}^{-1}$ corresponds to the ethylene adsorption on the surface of porous Materials whereas similar IR bands were absent in PAF-1-SO₃H and MIL-101-SO₃H suggesting the importance of Ag(I) in enhancing the ethylene adsorption. The blue shift in $-\text{CH}_2$ wagging mode in IR attributed to the combination of $d-\pi$ and $d-\pi^*$ interaction between Ag and ethylene. Controlled reduction of Fe^{3+} to Fe^{2+} was performed by activating MIL-101(Fe) at high temperature ($150\text{--}250^\circ\text{C}$) under vacuum (Yoon et al., 2010). The breakthrough experiments with equimolar mixture of propylene and propane clearly demonstrates $\text{C}_3\text{H}_6/\text{C}_3\text{H}_8$ selectivity of 26 suggesting the role of OMS. Selective adsorption of propylene over propane was reported in MOF-74-M (M = Mg, Co and Mn). Among three MOFs tested, MOF-74-Co was proven to have exceptional propylene/propane selectivity of 46 suggesting strong π complexation between propylene and Co(II) sites. Like MOFs, researchers also explored hyper cross-linked polymers (HCPs) doped with Ag(I) ions for efficient separation of propylene from propane. The column breakthrough experiments using equimolar mixture of propylene and propane suggest the propylene is preferentially adsorbed by Ag(I) doped HCP.

MIL-100(Fe) is one of the MOFs reported for propylene/nitrogen separation (Ribeiro et al., 2013). The MIL-100(Fe) with a 3D tetrahedron structure consists of Fe octahedra and oxo-central organic linker with two types of mesopore. MIL-100(Fe) has high propylene/nitrogen selectivity at 2.5 bar and 70°C , and since the propylene adsorption isotherm remains linear up to 2 bar, excellent working capacity of propylene can be obtained even with moderate pressure in the regeneration step. Most of the sorbents discussed above will bind olefin strongly because of the π complexation mechanism or pore walls functionalized with hydrogen bonding groups or size-exclusion mechanism. Overall N_2 weakly interacts with pore walls of the frameworks as a result of low adsorption capacity. Therefore, MOFs with open metal sites or pore size approximately the size of olefin kinetic diameter can be used to improve olefin/ N_2 selectivity.

In another study, eight different stable MOFs including microporous, mesoporous and functionalized MOFs were synthesized and tested for the selective separation of propylene over nitrogen. Among these MOFs, CAU-1, the ultramicroporous MOFs decorated with amine functional groups were reported to exhibit the highest IAST selectivity of 236 and 313, respectively, at 298 K and 273 K under atmospheric condition, which is greater than those of zeolite 5A and microporous carbon. The remarkable selectivity and high Q_{st} of propylene were attributed to the presence of a small tetrahedral cage of pore size 5 \AA and the amino functional groups. This is further confirmed by DFT calculations showing strong electrostatic interactions between the amino group and the C = C bond in propylene. Breakthrough experiments, stability and recyclability tests suggested that CAU-1 is an ideal adsorbent material for propylene/nitrogen separation in a typical industrial condition (Tan et al., 2019).

Styrene is usually obtained by the dehydrogenation of ethylbenzene. However, owing to the thermodynamic constraints, the reaction is not completed and hence a large amount of unreacted ethylbenzene always remains mixed with styrene. A MOF structure, Co-MOF-74, was reported with open metal sites (OMSs) that can separate the xylene isomers and C_8 aromatics, including ethylbenzene (Gonzalez et al., 2018). It is known that the unsaturated Co^{2+} site of Co-MOF-74 is capable of separating ethylbenzene by thermodynamic equilibrium owing to the different degree of interactions between each adsorbate and the adsorbent. However, it has a low selectivity in which it cannot fully separate styrene and ethylbenzene. It was found that ethylbenzene can be better separated by the size exclusion mechanism described in the section “separation based on size-exclusion”.

The successful report of π complexation in the other type of adsorbents has also been reported. The π -complexation of ethylene and propylene on Ag(I)-doped and micro-mesoporous carbons has been

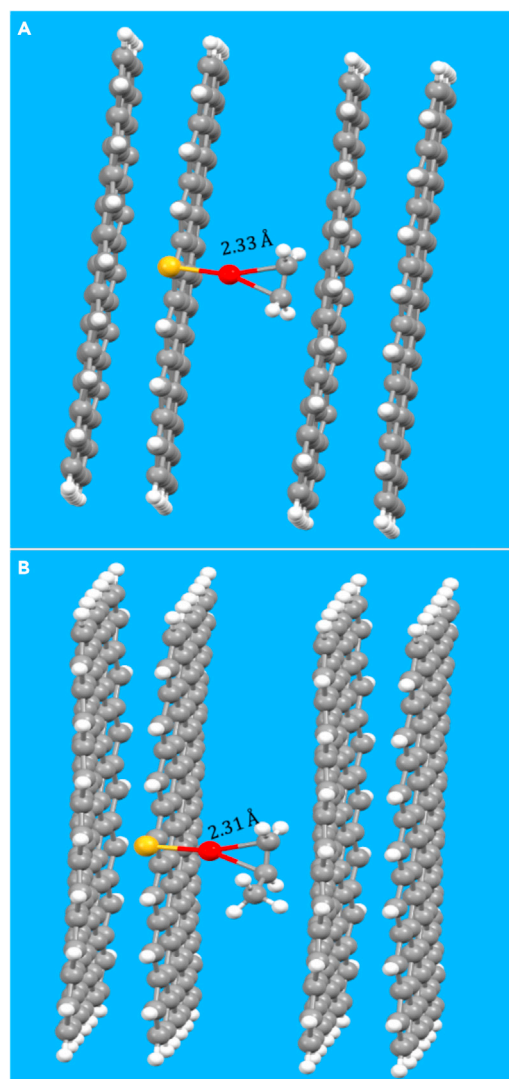


Figure 3. DFT calculation results revealing the bond formation between Ag(I) and π orbital of olefin on graphitic carbons surface

(A) Ag(I) and π orbital of ethylene.

(B) Ag(I) and π orbital of propylene, DeLuca et al., 202, Copyright 2021 Elsevier.

reported along with density function theory (DFT) to explain the fundamental chemistry. Ag(I) doping was enhanced by sulfurization of porous carbon that increased the selectivity of ethylene and propylene over ethane and propane, respectively (Saha et al., 2020; De Luca et al., 2021). DFT-based computation (De Luca et al., 2021) revealed that Ag(I) forms a bond with π -orbital of ethylene and propylene in the narrow slit shaped pores of width 5.23 Å. The calculated bond lengths were 2.33 Å and 2.31 Å for ethane and propane, respectively (Figure 3). It was also revealed that Ag(I) makes a bond with the π -orbital of sp^2 hybridized graphitic carbon on the opposite side of slit pore in the presence of ethane and propane thereby rejecting the alkane molecule. This phenomenon corroborates the selectivity of Ag(I) functionalized carbon to the alkene molecule, i.e., ethylene and propylene. The DFT calculation also revealed that the enthalpy of adsorption of ethylene and propylene is 6.1 to 3.6 times higher than that of ethane and propane, respectively, that further corroborates the selectivity of Ag(I)-doped carbon towards an alkene. Molecular orbital (MO) analysis revealed the partial overlap between π -orbital of an alkene and s or d -orbital of Ag(I) that supports the theoretical support of the π -complexation process. Cu(I)-doped and hard-templated mesoporous carbons (CMK-3) and surfactant templated mesoporous carbons were successfully reported as ethylene selective adsorbent for ethane/ethylene separation. Recently, Cu(I) doped mesoporous carbon

(Jiang et al., 2013), activated carbon (Gao et al., 2016) also reported to be an ethylene selective adsorbent and it was demonstrated that it can separate ethylene from the product mixture of oxidative coupling reaction of methane (OCM).

The π -complexation of olefins was successfully implemented for zeolite materials as well. Inclusion of additional materials within the zeolite framework was performed by ion exchange or dispersion method. CuCl dispersed faujasite zeolite (NaX) (Miltenburg et al., 2006) and Li^+ exchanged 13X (Grande et al., 2010) demonstrated successful separation of ethylene and propylene from their paraffin counterparts. The π -complexation has also been exploited by different types of lattice cations of zeolite-based materials, like, zeolite 13X (Schmittmann et al., 2020; Pu et al., 2018), ITQ-32 (Gutiérrez-Sevillano et al., 2010; Palomino et al., 2007) carbon-nanotube doped-ZSM-58 (Selzer et al., 2018) and aluminosilicates (Luna-Triguero et al., 2020). A systematic study was performed to understand the role of few metals in influencing π complexation in zeolite materials. In this work, seven metal ions, Ag, Na, K, Li, Cu, Ba, La and mixed metal and hydrogen ions of Ba/H and La/H were impregnated onto Engelhard Titanosilicate (ETS-10) (Anson et al., 2008) zeolite. The IAST-based adsorption selectivity of ethylene over ethane decreases in the order of $\text{Na} > \text{K} > \text{Li} > \text{Cu} \sim \text{Ba} > \text{Ba/H} > \text{La} > \text{H}$. Despite Ag and Cu demonstrated poor selectivity compared to other cations, they demonstrated a better gas swing capacity (for application in pressure swing adsorption, PSA) and rectangular type of ethylene adsorption isotherm demonstrating a better adsorbate-adsorbent interaction.

The π -complexation has also been successfully employed for different mesoporous silica materials, including Ag(I)/SBA-15 (Grande et al., 2004), Cu(I)/SBA-15 (Basaldella et al., 2006), Ag(I)/MCM-41 (Iucolano et al., 2008), Cu(I)/MCM-48 (Le et al., 2008). AgNO_3 -dispersed silica gel (Rege et al., 1998) and Cu(I) or Ag(I)-doped aluminosilicate materials (Kargol et al., 2004). Ag(I)-doped SBA-15 and MCM-41 showed the preferential adsorption of propylene over propane whereas Cu(I) doped MCM-48 demonstrated preferential adsorption of ethylene over ethane. Density function theory (DFT) was investigated to study the geometry of molecular moieties during adsorption and energetics of ethylene and propylene adsorption that further confirmed the presence of π -complexation (Jiang et al., 2006). The structural conformation revealed that Ag(I) is coordinated by the three hydrogen bonds between two oxygen atoms of silanol groups and one from the anion originating from silver salt. The electron density difference confirmed the partial transfer of electron from Ag 4d-orbital to the π orbital of ethylene forming the Ag- C_2H_4 bond along with hybridization of Ag 5s-orbital with the same π -orbital of ethylene. In the neighborhood of adsorbing atoms, the strongest binding energy is present between Ag and ethylene, which is 0.80 eV. The similar scenario was also observed between Ag(I) and propylene (Jiang et al., 2006) suggesting the similar π -complexation.

Hydrogen bonding

Hydrogen bonding is a type of weak chemical bond formation represented as $\text{X}-\text{H}\cdots\text{Y}$ in which a hydrogen bond is formed between hydrogen atom (H) and a foreign atom (Y). The energy of a hydrogen bond lies within 40 kcal mol^{-1} to $0.25 \text{ kcal mol}^{-1}$ depending on the electronegativity of X and Y, or in other words, degree of acidity of X and degree of basicity of Y. It has been well recognized that hydrogen bonds play a significant role in chemistry and biology. The hydrogen bond strength can be categorized in to partly covalent ($\text{O}-\text{H}\cdots\text{O}$, $\text{N}-\text{H}\cdots\text{O}$ etc.) to electrostatic ($\text{C}-\text{H}\cdots\text{O}$, $\text{N}-\text{H}\cdots\text{S}$ etc.) and partly van der Waals type ($\text{C}-\text{H}\cdots\pi$, $\text{C}-\text{H}\cdots\text{Cl}$, $\text{C}-\text{H}\cdots\text{FC}$ etc.) depending on how the hydrogen atom is connected to the system (Figure 4). The hydrogen atoms in olefins and paraffins possess different levels of acidity and it may be harnessed to switch the selectivity between olefins to paraffins or vice versa for a suitable adsorbent. For example, hydrogen atoms in C_2H_2 molecule ($\text{pK}_a = 26$) are more acidic compared to C_2H_4 ($\text{pK}_a = 45$) and C_2H_6 ($\text{pK}_a = 62$). As a result, C_2H_2 forms stronger hydrogen bonds with sorbent molecules over C_2H_4 , likewise C_2H_4 forms stronger hydrogen bonds over C_2H_6 . Similarly, C_3H_6 forms stronger hydrogen bonds with sorbents because of the higher acidic hydrogen atoms ($\text{pK}_a = 44$) over C_3H_8 ($\text{pK}_a = 50$). Several research groups have utilized these hydrogen bonds to design MOFs and hydrogen bonded frameworks for selective capture of olefins from paraffins and vice versa.

An excellent example for the role of hydrogen bonds for improved $\text{C}_3\text{H}_6/\text{C}_3\text{H}_8$ selectivity is observed in a MOF with metal azolate framework (known as MAF-23) using flexible linker (bis(5-methyl-1H-1,2,4-triazol-3-yl)methane (H_2btm)) (Wang et al., 2019a, 2019b). The pore size (3.6 \AA) in MAF-23 is smaller than many guest molecules; however, MAF-23 shows excellent performance towards C_4 hydrocarbon separation due to the flexible nature of the organic linker. Authors post-synthetically modified MAF-23 by oxidizing

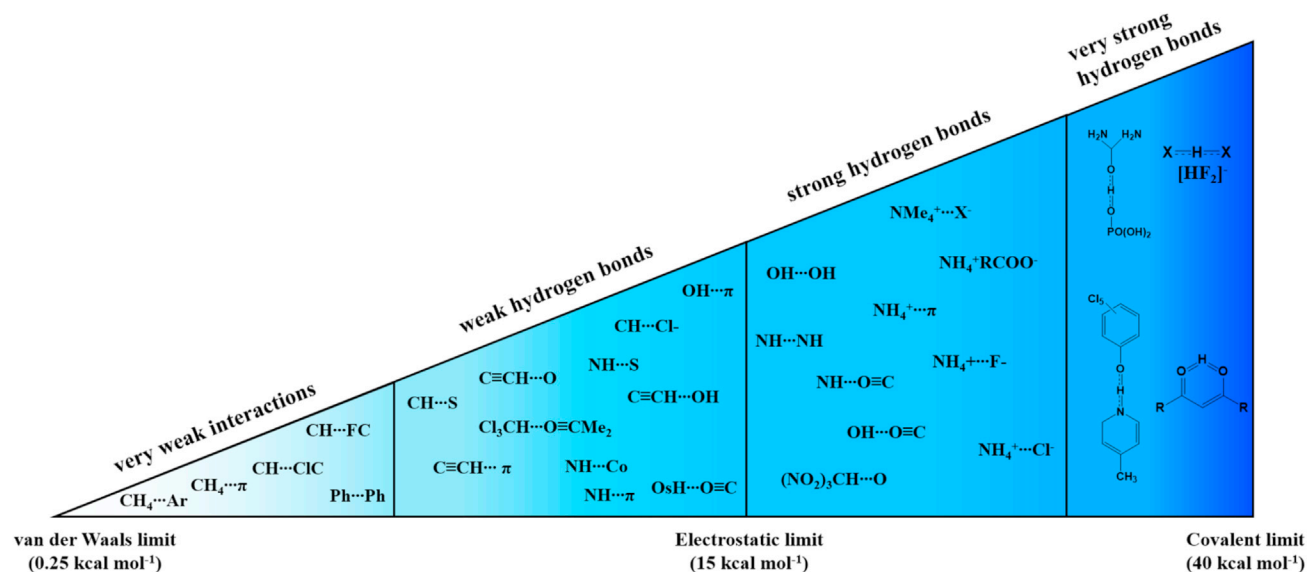


Figure 4. Elucidation of different types of hydrogen bonding strengths Modified from Desiraju, 2002.

highly acidic methylene (-CH₂) group in H₂btm to hydrophilic keto group (-C=O) to result in MAF-23-O. In MAF-23-O, the propylene breakthrough was much later (2.4 mmol g⁻¹) than propane (0.7 mmol g⁻¹) suggesting that after oxidation C₃H₈ adsorption was significantly reduced. The single-component adsorption experiments showed propylene adsorption uptake in MAF-23-O was 1.4 mmol g⁻¹, whereas propane was as low as about 1.1 mmol g⁻¹ at 1 bar and 298 K (Figure 5A). The IAST selectivity was calculated as 8–9 for MAF-23-O while 3–4 for MAF-23. The calculated binding energies for C₃H₆ in MAF-23-O was found to be 54 kJ mol⁻¹ compared to 34 kJ mol⁻¹ for propane. GCMC simulation confirmed that propane has large number of C-H...O hydrogen bonds compared to propylene but it was compensated by the highly acidic nature of hydrogen atoms in propylene that provided the strong host guest binding energy.

A series of isostructural MOFs was synthesized by using 4,4'-dipyridylacetylene as organic linker, copper metal node pillared with hexafluorosilicate (SiF₆²⁻) or hexafluorogermante (GeF₆⁻) anions forming a 3D network structure known as SIFSIX-2-Cu-i and GeFSIX-2-Cu-i (i = interpenetrated) (Wang et al., 2020). The pore apertures of GeFSIX-2-Cu-i and SIFSIX-2-Cu-i were found to be 4.5 and 4.7 Å, respectively. The GeFSIX-Cu-i shows high C₃H₆ capacity (2.69 mmol g⁻¹) compared to that of C₃H₈ (1.80 mmol g⁻¹) under identical conditions. Similarly, SIFSIX-Cu-2-i has slightly lower C₃H₆ capacity (2.65 mmol g⁻¹) compared to GeFSIX-2-Cu-i. The IAST selectivity values of C₃H₆/C₃H₈ on GeFSIX-2-Cu-i and SIFSIX-2-Cu-i were found to be 4 and 5 at 298 K and 1 bar, respectively. The density functional theory (DFT) simulations suggest the C₃H₆ molecule is bound by two GeF₆⁻ anions from different nodes via -C=H...F and C-H...F hydrogen bonds (2.127 Å and 2.377 Å) from C₃H₆. Similar interactions were found with C₃H₈ molecules. However, the acidity of hydrogen atoms in propylene is stronger than that of propane leading to stronger interaction between C₃H₆ and GeFSIX-2-Cu-i. Besides hydrogen bonds, π...π interactions between propylene and the pyridine ring was also found to strengthen the interaction between C₃H₆ and the framework of GeFSIX-2-Cu-i.

Similarly, hydrogen bonding interactions have been extensively used to separate acetylene from hydrocarbons by functionalizing the pore surface with electronegative atoms. An excellent performance of SIFSIX-2-Cu-i was reported for acetylene separation from ethylene (Cui et al., 2016). The remarkable C₂H₂ selectivity of SIFSIX-2-Cu-i was also shown in the breakthrough experiment, which results in 99.998% purity of C₂H₄ (Figure 5B). The first principle calculations and neutron diffraction experiments with C₂D₂ molecule suggested that C₂D₂ is strongly bound through the C-H...F hydrogen bonding and van der Waals interaction with organic linker. The SIFSIX-Cu-2-i contains four exposed F atoms and each exposed F atom binds to one C₂H₂ molecule through multiple H^{δ+}...C^{δ-} dipole-dipole interactions.

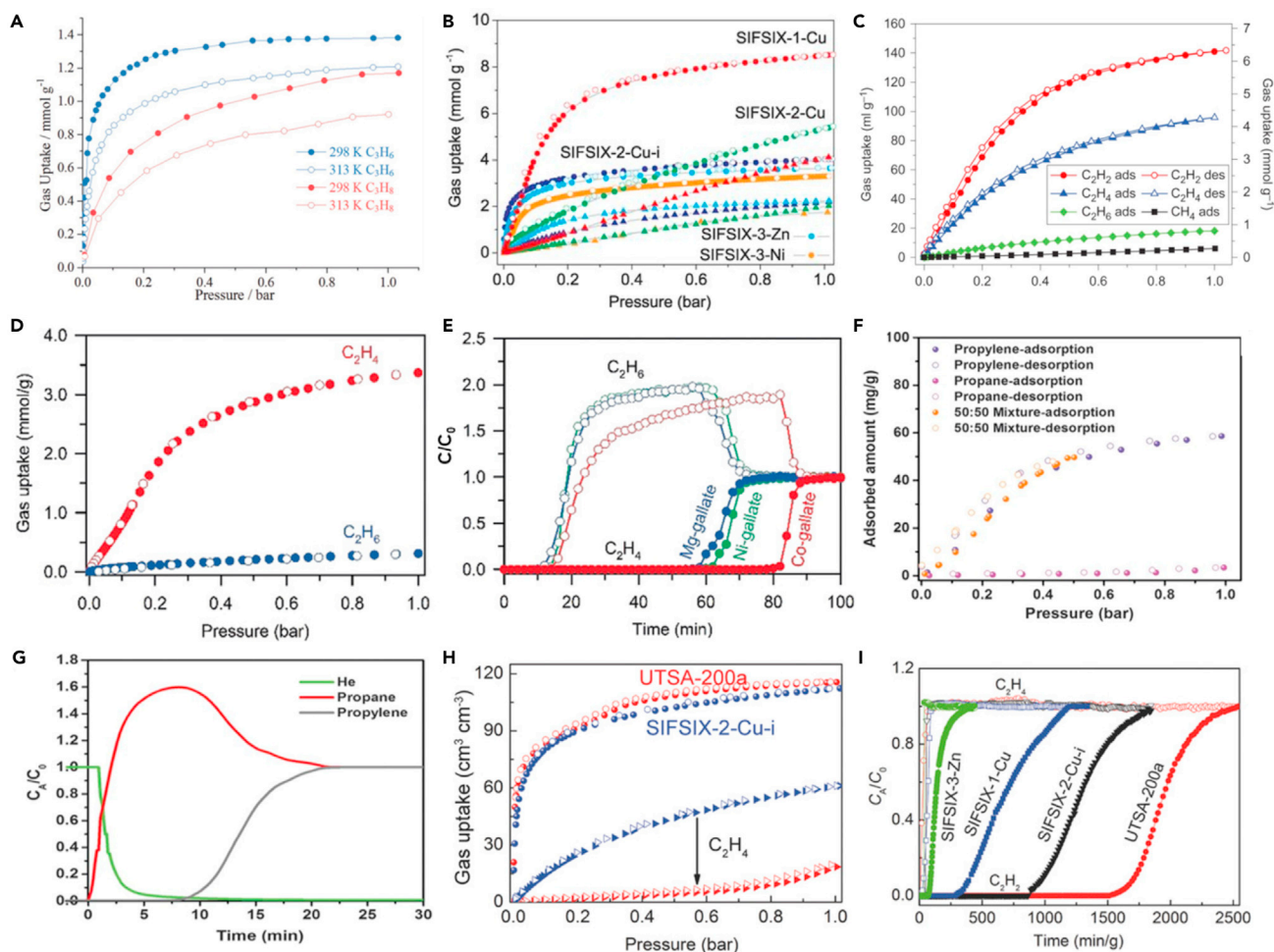


Figure 5. Adsorption isotherms on some MOFs

(A and B) MAF-23-O for propylene and propane adsorption isotherms (Wang et al., 2019a, 2019b) Copyright 2019, John Wiley and Sons (B) C_2H_2 (filled circles) and C_2H_4 (filled triangles) adsorption isotherms of the SIFSIX series at 298 K (Cui et al., 2016) Copyright 2016, The American Association for the Advancement of Science.
 (C) C_2H_2 , C_2H_4 , C_2H_6 and CH_4 adsorption isotherms in NOTT-300 at 293 K (Yang et al., 2015) Copyright 2014, Nature Publishing Group.
 (D) The single-component C_3H_8 (purple) and C_3H_6 (orange), and equimolar mixture of C_3H_6/C_3H_8 isotherms of KASUT-7 at 298 K (Cadiou et al., 2016) Copyright 2016, The American Association for the Advancement of Science.
 (E) The breakthrough experiment of KAUST-7 for C_3H_6/C_3H_8 equimolar mixture at 298 K (Cadiou et al., 2016) Copyright 2016, The American Association for the Advancement of Science.
 (F) Pure C_2H_4 and C_2H_6 adsorption isotherms of Co-gallate MOF at 298 K (Bao et al., 2018) Copyright 2018, John Wiley and Sons.
 (G) The breakthrough curves of M-gallate MOFs (M = Co, Mg, and Ni) for the equimolar C_2H_4/C_2H_6 mixture at 273 K (Bao et al., 2018) Copyright 2018, John Wiley and Sons.
 (H) Pure C_2H_2 (circles) and C_2H_4 (triangles) adsorption isotherms of UTSA-200a (red) compared with SIFSIX-2-Cu-i (blue) (Li et al., 2017a, 2017b) Copyright 2017, John Wiley and Sons.
 (I) The breakthrough curves for C_2H_2/C_2H_4 mixtures with UTSA-200a, SIFSIX-2-Cu-i, SIFSIX-1-Cu, SIFSIX-3-Zn at 298 K. (Li et al., 2017a, 2017b) Copyright 2017, John Wiley and Sons

MUF-17 (MUF = Massey University Framework) possesses one-dimensional zig-zag channels that are lined with amino and carboxylate group and coordinated water molecules can separate both bulk and trace acetylene from ethylene and carbon dioxide mixtures. For instance, at 293 K and 1.0 bar, the C_2H_2 uptake is 3.01 mmol/g, whereas the C_2H_4 and CO_2 uptake are 2.15 mmol/g and 2.51 mmol/g respectively. Similarly, at low pressure 0.01 bar, C_2H_2 uptake is more than double that of C_2H_4 and CO_2 . Based on pure component isotherms at multiple temperatures, adsorption enthalpies (Q_{st}) were evaluated to determine the binding strength between the framework and guest molecules. A very high Q_{st} value was reported for

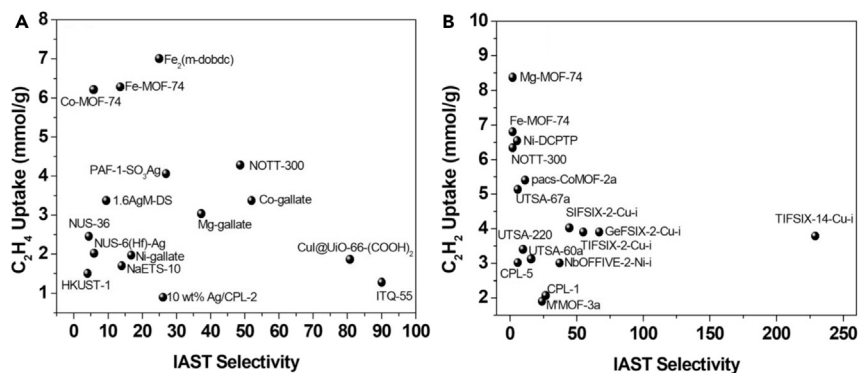


Figure 6. IAST calculated selectivity versus pure component uptake plot

(A and B) 1:1 (v/v) mixture of C₂H₄:C₂H₆ and (B) 1:99 (v/v) mixture of C₂H₂:C₂H₄ for some of the selective MOFs at 1 bar and room temperature.

C₂H₂ (49.5 kJ/mol) when compared to C₂H₄ and CO₂, respectively at zero loading. To gain further insight into the mechanism of adsorption, DFT-D3 calculations were performed to identify the preferential binding sites of the guest molecules in MUF-17. Consistent with the Q_{st} values, C₂H₂ form strong interactions with the framework. The polar hydrogen atom of C₂H₂ interact with the coordinated oxygen atoms of a framework carboxylate group through C≡C●●●O hydrogen bonding with a distance of 2.34 Å. In addition, the negative carbon atom of C₂H₂ molecule interacts with a hydrogen atom of an amino group, with a distance 2.46 Å, much shorter than the sum of van der Waals radii of hydrogen (1.20 Å) and carbon (1.85 Å). Similar geometry is observed for C₂H₄ guest molecule despite a significantly weaker interactions with the framework. Both the size and the electrostatic interaction between the guest molecule and the framework play a crucial role in distinguishing C₂H₂ and C₂H₄ with a large adsorption enthalpy difference (Qazvini et al., 2019a, 2019b).

These sets of examples show the importance of hydrogen bonding interactions between host and guest along with appropriate pore size to improve C₂H₄/C₂H₆, C₂H₂/C₂H₄ and C₃H₆/C₃H₈ selectivity. Furthermore, Figure 6 shows the IAST calculated selectivity and the individual component uptake for gas mixtures C₂H₄/C₂H₆ and C₂H₂/C₂H₄ in some of the top performing MOF materials at 1 bar. As seen in Figure 6, there is a tradeoff between the uptake and selectivity values i.e., MOF with higher selectivity is reported to have lower uptake capacity and vice versa. Hence developing high-performance materials having both high uptake and selectivity is desirable (Zhang et al., 2020; Chen et al., 2021; Zhu et al., 2021).

A hydroxy functionalized MOF known as NOTT-300 was reported for ethylene and ethane adsorption by harnessing hydrogen bonding (Yang et al., 2015). The single-component gas adsorption suggested that NOTT-300 possessed higher adsorption capacity toward C₂H₄ (4.28 mmol g⁻¹) compared to C₂H₆ with an adsorption capacity of 0.85 mmol g⁻¹ significantly lower than C₂H₄ at 1 bar and 293K (Figure 5C). The IAST calculation shows the selectivity of 48.7 higher than MOFs with open metal sites including HKUST-1 (4.0), MOF-74-Co (6.0), MOF-74-Fe (13.6) and PAF-1SO₃Ag (27). The *in-situ* synchrotron powder X-ray diffraction experiments reveal that the M-OH groups and phenyl rings in NOTT-300 involved in multiple C-H●●●O and C-H ... Pi interactions with adsorbed C₂H₄. The C₂H₄ molecule is about 4.62 Å (C●●●O) away from M-OH group whereas C₂H₆ molecule is further away from the M-OH group with C●●●O distance of 5.07 Å.

Hydrogen bonding along with molecular sieving was responsible for separation of propyne from propylene in a flexible MOF composed of [Cu(bpy)₂(OTf)₂] (bpy = 4,4'-bipyridine, OTf⁻ = trifluoromethanesulfonate) known as ELM-12 (elastic layered structured MOF, ELM) (Li et al., 2017a, 2017b). It possesses dumbbell (6.1 Å × 4.3 Å × 4.3 Å) and ellipsoid-shaped (6.8 Å × 4.0 Å × 4.2 Å) pores, which are separated by dynamic OTf⁻ groups. The pores in ELM-12 are close to the molecular size of propyne molecules. The single-component adsorption experiments on ELM-12 showed exceptional uptake towards C₃H₄ (2.55 mmol g⁻¹) compared to C₃H₆ (0.67 mmol g⁻¹) at 298K and 0.1 bar, resulting in IAST selectivity of 84 and 279 for 1/99 and 50/50 mixture of propyne and propylene, respectively. The neutron diffraction experiments

suggested that the C_3H_4 molecule has a relatively strong hydrogen bonding ($C-H \cdots O$) with the OTf^- groups and the dynamic OTf^- group changes the pore by adjusting its position according to the C_3H_4 loading. Therefore, a high C_3H_4 selectivity of ELM-12 can be described as a molecular sieving effect coupled with strong hydrogen bonding between C_3H_4 and ELM-12 inside the framework.

Separation based on pore morphology

Separation based on size-exclusion

Pore size and shape of porous materials play a critical role in many gas separations. Traditionally, size and shape-based separations were commonly observed in zeolite (zeolite 3A and 5A) and carbon molecular sieves (CMS). Separation based on size-exclusion, often referred to as steric separation, incorporates the rejection of one or more molecules, which are larger than the pore opening of the adsorbent material. If successful, this type of separation generally provides higher efficiency and purity of the separated products compared to other mechanisms. Besides a few handfuls of adsorbents, it is quite challenging to obtain a desired and specific pore size within the adsorbents in traditional types of adsorbents such as zeolites and carbons. On the other hand, pore sizes and shapes of MOFs can be controlled quite precisely by the choice of organic linkers, and metal clusters present in their crystals. MOFs can also be post-synthetically modified to control pore size to exclude one molecule over the other. As mentioned earlier, owing to the very similar size of the hydrocarbon molecules, it is highly necessary to precisely control the pore size and shape of the MOFs to utilize the separation by size exclusion mechanism. If successfully controlled, the unique geometry of pores in the MOFs can be a powerful tool to efficiently separate the hydrocarbons with a diameter difference of less than 0.5 \AA . Several articles were published on controlling the pore size of MOFs to separate olefins from other hydrocarbons and we provided a short glance on a few of the prominent articles in the sections below.

A Co-gallate MOF was synthesized using gallic acid with a pore aperture of 16.8 \AA^2 which is slightly larger than the C_3H_6 (16.4 \AA^2) and smaller than C_3H_8 (21.2 \AA^2), indicating a potential for molecular sieving effect (Liang et al., 2020). Single component C_3H_6 and C_3H_8 adsorption suggest on Co-gallate MOF shows a C_3H_6 uptake capacity of $66.6 \text{ cm}^3/\text{g}$ (STP) at 1 bar which is higher than other M-gallate ($M = Ni$ and Mg) MOFs. In contrast, Co-gallate MOF has an extremely small amount of C_3H_8 uptake ($5.2 \text{ cm}^3/\text{cm}^3$, STP) which is several orders of magnitude lower capacity than those of $M_2(\text{dobdc})$ or $M_2(m\text{-dobdc})$ discussed earlier. The higher C_3H_6 adsorption capacity and lower C_3H_8 capacity of Co-gallate MOF results in exceptional selectivity towards C_3H_6/C_3H_8 separation compared to other MOFs. To further demonstrate the selectivity, the dynamic breakthrough experiments with 50%/50% mixture of C_3H_6/C_3H_8 show longer retention time for propane (28 min) compared to that of C_3H_8 . To elucidate the mechanism, the neutron powder diffraction experiments with C_3D_6 molecules suggest the C_3D_6 molecule is stabilized inside the pore walls of the Co-gallate MOF through strong and weak hydrogen bonding including $C-D \cdots O$, $O-H \cdots \pi$ and $C-D \cdots \pi$ interactions between C_3D_6 molecules and hydroxyl/aromatic rings of the ligand. The combination of pore size and hydrogen bonding between C_3H_6 and Co-gallate MOF enable the selective separation of these closely related molecules with exceptional selectivity.

KAUST-7 (also known as NbOFFIVE-1-Ni) is a family of ultra-micro porous materials constructed using 2D square grid composed of pyrazine linked with nickel nodes that are pillared via inorganic building blocks ($NbOF_5^-$) in the third dimension to obtain a periodic net with cubic topology (Wang et al., 2018a, 2018b). The KAUST-7 is the structural analogue of the previously reported SIFSIX class of MOFs. The previously reported SIFSIX-3-M ($M = Cu, Ni$ and Zn) exhibits direct CO_2 capture from air; however, it was unable to adsorb the olefin/paraffin mixtures, like, propane and propylene, owing to its larger pore apertures ($5\text{--}7 \text{ \AA}$). Eddaoudi and co-workers down sized the pore aperture ($3\text{--}4.8 \text{ \AA}$) by replacing the SiF_6^{2-} pillars with SIFSIX-3-Ni with larger $NbOF_5^{-2}$ pillars. The pore aperture in KAUST-7 found to be optimum for separating propane and propylene. Based on single component adsorption, KAUST-7 allowed the adsorption of C_3H_6 but restricted C_3H_8 because of the unfavorable pore size. The propylene adsorption uptake was found to be 2.7 mmol g^{-1} at 1 bar and 298 K, and propane was negligibly adsorbed (Figure 5D). The equimolar mixed gas adsorption along with breakthrough experiments suggests a complete molecular exclusion of propane from propylene using KAUST-7 (Figure 5E). In addition, the gas uptake capacity and size-exclusion were fully maintained even after 10 cycles of adsorption and desorption.

The Yttrium-based Y-abtc (abtc: 3,3',5,5'-azobenzene-tetracarboxylates) MOF has been developed along with three other MOFs by combination of Zr_6 and Y_6 secondary building units (SBUs) and two organic linkers

(bptc (3,3',5,5'-biphenyltetracarboxylates) and abtc) (Wang et al., 2018a, 2018b). Amongst these three MOFs, Y-abtc has the optimal pore size that can only adsorb propylene and exclude propane completely. The pore sizes in Zr-abtc and Zr-bptc are large enough to adsorb both propylene and propane. On the other hand, the pore aperture in Y-bptc is too small to adsorb either propylene or propane. Multi component breakthrough experiments using Y-abtc reveal the material can produce propylene with 99.5% purity.

Similar to propylene-propane separation, separation of ethylene from ethane was also studied using a size-exclusion mechanism in a cobalt-based gallate MOF capable of selectively separating ethylene from ethane (Bao et al., 2018). The gallate-based MOFs have a zig-zag shaped channel with pore sizes of 3.47–3.69 Å that is smaller than the kinetic diameters of ethylene and ethane. However, the pore size of the MOF is larger than the molecular cross-section of ethylene (3.28 Å) but smaller than that of ethane (3.81 Å). In this unique pore architecture, ethylene can diffuse through the pore channel to become selectively adsorbed whereas ethane can be rejected. This MOF showed equilibrium ethylene uptake capacity of 3.37 mmol g⁻¹ at 1 bar and 298 K, unlike 0.3–0.4 mmol g⁻¹ of ethane under the same conditions (Figure 5F). The breakthrough test of M-gallate MOFs (M = Co, Mg, and Ni) for C₂H₄/C₂H₆ mixture showed that all M-gallate MOFs can completely separate C₂H₄ and C₂H₆, and the adsorbed C₂H₄ can be easily desorbed by helium or vacuum (Figure 5G). The same research group reported a MOF that could completely exclude ethane compared to ethylene by adjusting the pore size/shape (Lin et al., 2018a, 2018b). Consisting of a 1D channel of robust organic ligand, UTSA-280 has a cross-sectional area of 14.4 Å². Therefore, it can only allow entry of ethylene, which has a relatively small cross-sectional area (13.7 Å²) compared to that of ethane (15.5 Å²). The ethylene adsorption capacity of UTSA-280 is 2.5 mmol g⁻¹ at 1 bar and 298 K, but ethane adsorption is negligible (0.098 mmol g⁻¹). UTSA-280 has demonstrated the pure ethylene productivity of 1.86 mol kg⁻¹ in a breakthrough experiment under dynamic mixture flow.

Similar size-exclusion strategy was further extended to exclude ethylene from the mixtures of acetylene and ethylene by reducing the pore size of the adsorbent in an ultra-microporous MOF. In this study, MOF structure was created using a shorter 4,4'-azopyridine (zapy, length 9.0 Å) organic linker with copper metal node and SiF₆²⁻ pillars to obtain SIFSIX-14-Cu-i (also known as UTSA-200) instead of 4,4'-dipyridylacetylene (dpa, length 9.6 Å), which was used in SIFSIX-2-Cu-i (Li et al., 2017a, 2017b). The SiF₆²⁻ and pyridine rings are connected via C–H···F hydrogen bonding to restrict the rotation of pyridine rings that result in the pores size of 3.4 Å in UTSA-200. Such a unique pore size is smaller than the kinetic diameter of C₂H₄ (4.2 Å) but larger than that of C₂H₂ (3.3 Å). The single-component C₂H₂ and C₂H₄ adsorption indicate that UTSA-200 adsorbs C₂H₂ with a very steep uptake (116 cm³ cm⁻³) at 1 bar and 298 K. On the other hand, UTSA-200 almost rejects C₂H₄ (0.24 mmol g⁻¹) because of the reduced pore size (Figure 5H). The IAST calculation suggested the selectivity of over 6000 at 1 bar and 298 K for binary mixtures of C₂H₂/C₂H₄ (1/99, v/v). In addition, the results of breakthrough experiments for C₂H₂/C₂H₄ separation under industrial process conditions showed that UTSA-200a has the potential to effectively separate C₂H₂ and C₂H₄ compared to other SIFSIX materials (Figure 5I). The exceptional selectivity arises from the small pore size in UTSA-200 along with C–H···F interactions with acetylene and SiF₆²⁻ pillars. The molecular exclusion of C₂H₄ has also been observed in different other MOFs, like UTSA-100, UTSA-200, ELM-12 and JCM-1 by precisely reducing the pore size with the help of organic linkers, metal nodes, inorganic pillars or functionalization of the pore walls to harness the hydrogen bonding groups resulting in further improvement of C₂H₂ uptake capacity and C₂H₂/C₂H₄ selectivity.

Given the subtle differences in the molecular size and shape of C₈ hydrocarbons, styrene and ethylbenzene can be separated via size-exclusion mechanism as well (Dey et al., 2021). A copper-based flexible MOF, named MAF-41 can undergo structural changes when guest molecules approach (Zhou et al., 2019). MAF-41 was proven to adsorb 2.31 mmol g⁻¹ of styrene at 298 K and 1 bar, whereas the adsorption of ethylbenzene is negligibly smaller. The size of ethylbenzene is excluded because it is too large to fit in the pores of MAF-41. This phenomenon results in the selective separation of styrene by molecular sieving effect with highly pure styrene (99%). It is generally claimed that the separation of C₈ hydrocarbons by size-exclusion is an ideal separation mechanism because it provides high adsorption selectivity, excellent efficiency and large energy-savings.

Apart from size – exclusion mechanism, the selectivity of styrene over ethylbenzene is driven by either enthalpic and/or entropic effects at saturation conditions, such as commensurate freezing, size entropy, length entropy, commensurate stacking and face-to-face stacking. A computational screening study was

done based on Configurational Bias Continuous Fractional Monte Carlo (CB/CFCMC) method on a series of MOFs with different topology and pore channel including MAZ, AFI and DON zeolites (1D-channel), MIL-47, MIL-53 and MAF-X8 (rhombohedral channels), and MOF-CJ3 respectively, to examine the separation mechanism of styrene and ethylbenzene mixture at 433 K. Size – exclusion effect is found at saturation condition in MFI zeolite where strong styrene selectivity occurs. However, in MAZ, AFI and DON zeolite structures and MIL-53 MOF, face-to-face stacking is observed where the molecules undergo a molecular reorientation to fit the channel dimensions favoring styrene selectivity. In both MIL-47 and MAF-X8 structures, commensurate stacking, which favors styrene molecules with stacking arrangements that are commensurate with the dimensions of 1D channels is observed at both low and saturation conditions. Among several mechanisms, commensurate stacking offers the best mechanism for the separation of styrene and ethylbenzene as well as the best trade-off between saturation capacity and selectivity (Torres-Knoop et al., 2015).

Separation based on gate-opening

MOFs, with their combination of inorganic metal subunits and organic ligands, have a multitude of variations that can lead to unique interesting properties. A particular subset of MOFs, known as the flexible MOFs, possesses a specific property that makes it very useful in the adsorptive separation of gases. The flexible MOFs can undergo phase transformations resulting in an alteration of the shape and size of their pores in response to the external stimuli, such as temperature, pressure, and, most importantly, interactions with guest molecules. The two most notable transformations of MOFs in the course of the gas separation are known as gate-opening and breathing effects. In a gate-opening transformation, a MOF can open its porous structure in response to external stimuli, i.e., a specific gas molecule, to transfer from a non-porous structure to a porous structure. This transformation allows the MOF to adsorb the same gas molecules that aided in this transition, thereby allowing its selective uptake from its mixture with other entities. This effect also facilitates the diffusion of the gaseous entity onto the inner core of the MOF thereby increasing the overall uptake capacity. These two transformations are often desirable to perform some specific selective gas separations.

A flexible MOF, named as RPM3-Zn, was employed for the selective separation of hydrocarbons by gate-opening mechanism (Nijem et al., 2012). RPM3-Zn was made from the ligands of 4,4'-biphenyldicarboxylate (bpdc) and 1,2-bipyriylethylene (bpee). The authors employed Raman spectroscopy and van der Waals density functional (vdW-DFT) to elucidate the gate-opening mechanism. It was observed that when ethane is incorporated within the MOF structure, its -CH₃ groups would form a weak hydrogen bond with the non-coordinated C=O bond of the bpdc ligand. It would also cause the dihedral angle originating from the two rings in bpdc to decrease resulting in gate opening effect. In this MOF, hydrogen bonding between adsorbate and adsorbent plays a unique role in the gate opening phenomenon. In the case of ethylene, the hydrogen bond may form not only with the noncoordinated C=O of the bpdc ligand, but also with the C=C and the C-C bonds along with the two rings. This latter interaction enormously increases the dihedral angle of the rings compared to what was caused by an ethane molecule. Because of such additional hydrogen bonding, the gate-opening pressure for ethylene was found to be higher than that of ethane that potentially allows the selective adsorption of ethane from the mixture of ethane and ethylene.

Selective adsorption of 1,3-butadiene from other C₄ hydrocarbons was demonstrated in a flexible MOF (Ye et al., 2017; Liao et al., 2017). In this study, the group synthesizes a MOF by reacting a ditopic ligand of 4-(3,5-dimethyl-1H-pyrazol-4-yl) benzoic acid (H₂mpba) with the Zn (II) salt of Zn(NO₃)₂·6H₂O. This group of researchers was able to create a unique MOF structure with this ligand and metal center by using toluene as a template that also served as a guest molecule to uniquely control the pore size by its presence. Toluene from the cavities of this MOF can be removed by heating, which results in smaller pores and channels. Interestingly, the pristine structure of this MOF can be restored by exposing it to toluene thereby showing the unique structural flexibility of this MOF. This MOF demonstrates atypical step-wise adsorption isotherms of N₂ and CO₂ with three consecutive stages. Those steps indicate the three stages of expansion of the structure thereby generating the breathing effect. This group of researchers examined the capability of toluene-free MOF to adsorb different C₄ hydrocarbons, namely n-butane, n-butene, isobutane, isobutene, and 1,3-butadiene. They discovered that each hydrocarbon was adsorbed with a different degree of gate-opening effect. The order of the adsorption was 1,3-butadiene < n-butene < n-butane < isobutene < isobutane. This also determined that the order is linked to the smallest cross-section of each molecule. The hydrocarbons can start getting adsorbed as soon as the gate opens enough for each hydrocarbon to orient

its smallest cross-section through the pore which combines the gate-opening mechanism with a size-exclusion mechanism.

An anion pillared flexible MOF known as TIFSIX-14-Cu-i, similar to SIFSIX and GeFSIX, can selectively capture propyne from propylene (Yang et al., 2018a, 2018b). TIFSIX-Cu-i is made up of 2D square grid nets composed of copper metal nodes coordinated with 4,4'-azopyridine bridged with TiF_6^{2-} anion pillars in third dimension. The unique chemistry of hybrid ultra-microporous materials allowed to fine tune the aperture size at a very narrow scale (0.1–0.2 Å) which makes it adequate for olefin/paraffin separation. Single-component propyne adsorption suggest both TIFSIX-14-Cu-i and GeFSIX-14-Cu-i show gate opening behavior; however, the TIFSIX-14-Cu-i showed fast response toward propyne which was reflected in gate-opening pressure of 500 ppm compared to that of 1,330 ppm for GeFSIX-14-Cu-i. The TIFSIX-14-Cu-i not only has a high propyne adsorption uptake (2.18 mmol g⁻¹) at low pressure (<0.01 bar) compared to SIFSIX-2-Cu-i and GeFSIX-14-Cu-i, but also showed a high propyne/propylene selectivity of 355 at 1 bar. The DFT simulations suggested that the pyridine ring was entitled to expand the channel in TIFSIX-14-Cu-i as soon as propyne was introduced whereas the GeFSIX-14-Cu-i has more restricted ring rotation resulting in a greater hindrance towards propyne. As a result, GeFSIX-14-Cu-i requires a high pressure to accommodate the propyne molecule (1,300 ppm). Furthermore, the propyne was stabilized by strong hydrogen bond $\text{-C}\equiv\text{C}\cdots\text{H}\cdots\text{F}$ and $\text{C}\cdots\text{H}\cdots\text{F}$ between C_3H_4 and TIFSIX-14-Cu-i. The IAST calculation suggested TIFSIX-14-Cu-i exhibit highest $\text{C}_3\text{H}_4/\text{C}_3\text{H}_6$ (1/99) selectivity of 355 compared to 217 (GeFSIX-14-Cu-i) and 41 (SIFSIX-14-Cu-i) under the identical conditions. Owing to this propyne affinity, TIFSIX-14-Cu-i shows great separation performance in breakthrough experiments under dynamic conditions.

Diffusion and kinetics-based separation

Diffusion or kinetics-based separations is a unique type of separation mechanism. Unlike affinity or size exclusion-based separation, equilibrium adsorbed amount is not the key factor to achieve such separation; instead, the difference in diffusivity values of gaseous components is harnessed to achieve the desired separation (Do, 1998). Although kinetic separation has been used for a long time to separate air in a commercial scale, application of such technique to separate olefins is rather few.

In the micropore domain, the intracrystalline diffusivity may be related to adsorbed amount by a well-known equation (Ruthven, 1984),

$$1 - \frac{m_t}{m_\infty} = \frac{6}{\pi^2} \sum_{n=1}^{n=\infty} \frac{1}{n^2} \exp\left(\frac{-\pi D_c t}{r_c^2}\right) \quad (\text{Equation 3})$$

This equation is often applied for one-term approximation and given as (Saha et al., 2008; Saha and Deng, 2010)

$$1 - \frac{m_t}{m_\infty} = \frac{6}{\pi^2} \exp\left(\frac{-\pi^2 D_c t}{r_c^2}\right) \quad (\text{Equation 4})$$

where m_t is the amount adsorbed at time t , m_∞ is the saturation uptake, r_c is the intracrystalline radius and D_c is the intracrystalline diffusivity. D_c/r_c^2 is referred to as diffusive time constant. The kinetic selectivity (S_k) based on the difference in intracrystalline diffusivity may be calculated as (Lee et al., 2011; Saha et al., 2017),

$$S_k = \frac{(D_c/r_c^2)_i}{(D_c/r_c^2)_j} \quad (\text{Equation 5})$$

where i and j are the faster and slower moving components, respectively.

The effective kinetic diffusivity (S) may also be defined as (Liu et al., 2015, 2017)

$$S = \frac{K_1}{K_2} \sqrt{\frac{D_1}{D_2}} \quad (\text{Equation 6})$$

where "1" and "2" are the faster and slower diffusing species, K is the Henry's constant and D is the intracrystalline diffusivity. The K -values may be obtained from the linear portion of the isotherms.

The self-diffusivity of ethane and ethylene within pure Si chabazite (Si-CHA) was measured by pulsed field gradient (PFG) nuclear magnetic resonance (NMR) spectroscopy (Hedin et al., 2008). Within

the (3.70 Å × 4.17 Å) pore Si-CHA, it was observed that self-diffusivity of ethane and ethylene at 101.3 kPa and 300.1 K are $0.48 \times 10^{-8} \text{ cm}^2 \text{ s}^{-1}$ and $3.1 \times 10^{-8} \text{ cm}^2 \text{ s}^{-1}$ respectively. Such a difference of diffusivity can denote the possible kinetic separation of those gases. In other work, the ratio of diffusivity of propylene to propane in Si-CHA and DD3R zeolite was reported to be as high as 10^4 suggesting a kinetic separation of those materials (Ruthven, 1984). Carbon molecular sieves (CMS) synthesized from different sources demonstrated kinetic separation of propylene over propane (Liu et al., 2015, 2017). CMS was synthesized by the carbonization of cation exchange resin of monosulfonated polystyrene crosslinked by monosulfonated divinylbenzene and polyvinylidene chloride (PVDC). It was reported that effective micropore size that influenced the kinetic separation was controlled by the crystallinity of precursor and pyrolysis temperature, whereas the crystallinity was dominated by the comonomer type and content. The propylene and propane diffusivities were $1.0 \times 10^{-9} \text{ cm}^2/\text{s}$ and $1.1 \times 10^{-11} \text{ cm}^2/\text{s}$, respectively, at 100 kPa and 90°C. This high ratio was suitable for the propylene/propane separation by kinetic methods. It was also reported that the kinetic selectivity, recovery and working capacity was better for CMS material compared to that of zeolite 4A. In another work, zeolite 4A and carbon molecular sieves were also employed for ethane/ethylene and propane/propylene separation (Rege et al., 1998).

A good example of separation of propylene by kinetics in MOF-based material was reported with the modification of MOF TO consisting of Zn(II) as secondary building units and 1,2,4,5 tetrakis (carboxyphenyl)benzene and tans-1,2-dipyridylethene struts (Lee et al., 2011). The four modified MOF structures that were created are DTO, DBTO and BTO, where D and B indicate deprotonated acetylene containing strut and dibrominated strut, respectively. It was reported that DBTO and BTO possess the superior kinetic selectivity of propylene over propane of 11 and 12, respectively, compared to that of parent MOF, TO (2.5). DTO demonstrated an inferior kinetic selectivity (1.4). In all those structures, the intracrystalline diffusivity of propylene was one order of magnitude lower compared to that of propane. In a separate work, A mixed linker MOF consists of benzotriazole (BTA) and benzimidazole (BIM) as linkers and Zn metal centers with BTA/BIM ratio 4/1 demonstrated kinetic separation of ethane and ethylene (Lyndon et al., 2020). Kinetic separation has also been performed for propane/propylene separation by zeolite imidazolate framework (Li et al., 2009).

Paraffin selective adsorbents for olefin separation

Despite the largest volume of research has been directed towards developing the olefin selective adsorbents that mostly harnesses the π -bond complexation or size-exclusion separation, it has been claimed that paraffin selective adsorbents can produce the polymer grade olefin easily and at a lower cost. In an adsorption column containing olefin selective adsorbent, olefin remains adsorbed in the column, whereas paraffin comes out from the other end of the column. In the course of desorption, olefin is contaminated with the paraffin that is present in the mobile phase. Therefore, to obtain the high purity olefin, a large number of cycles are usually necessary, which increases both the cost and energy-input of the process very heavily. On the other hand, a paraffin selective adsorbent can transfer the olefin to the mobile phase, thereby minimizing the possibility of paraffin contamination. Such an ethane selective adsorbent may not require multiple separations steps to obtain polymer-grade olefin.

The readers should be aware that selectivity towards paraffin for olefin separation does not involve any new mechanism of separation. All the mechanisms explained earlier, except π -complexation and OMS can be harnessed to generate paraffin selectivity of an adsorbent, depending on how a specific adsorbent has been designed and synthesized.

A flexible MOF ZIF-7 was reported to separate ethane and ethylene by using a gate-opening mechanism (Gücüyener et al., 2010). In ZIF-7, the gate-opening pressure for ethane is lower than that of ethylene. It can be attributed to the fact that the three-lobe shaped pores allow ethane and its three-fold symmetric methyl group to better interact with the pore surface of the adsorbent decorated with benzene rings. Thus, the enhanced interaction between ethane and pore surface allows the pore mouth to open at a lower pressure compared to that of ethylene causing superior adsorption of ethane under the same conditions of temperature and pressure. Similar effect was also responsible for elevated adsorption of propane compared to that of propylene, but to a smaller extent, owing to the additional methyl group present in propane molecules. The breakthrough experiments with ZIF-7 demonstrated a delayed release of ethane at a pressure higher than the gate-opening pressure of ethylene thereby suggesting that the MOF could still retain its selectivity to ethane at the elevated pressure. Further work combining DFT calculations and

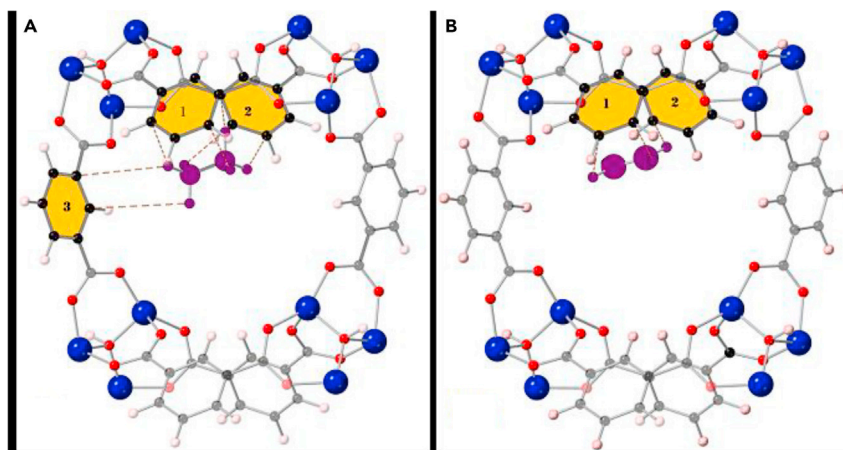


Figure 7. Comparison of the preferential

(A and B) C_2H_6 and (B) C_2H_4 adsorption sites in MUF-15 identified from the DFT – D3 calculations (Co, blue; O, red; C, gray; H, pastel magenta),

thermodynamic analysis of the adsorption – desorption isotherms elucidated the gate opening mechanism underlying the ethane selectivity in ZIF-7. DFT calculations based on a cluster model showed that both C_2H_6 and C_2H_4 interactions are dispersive in nature, slightly higher in C_2H_6 , which is attributed to the larger number of $CH \cdots \pi$ interactions. In addition, DFT computed energy profiles revealed the subtle difference in the way they form adsorption complex with external surface, where ethene adsorption causes a significant distortion of the ZIF-7 cage structure, thereby blocking the cage entrance (Van Den Bergh et al., 2011).

A MOF structure with iron(III) peroxide 2,5-dioxido-1,4-benzenedicarboxylate [$Fe_2(O_2)(dobdc)$ ($dobdc^{4-}$: 2,5-dioxido-1,4-benzenedicarboxylate)] was reported as an ethane selective adsorbent (Li et al., 2018). The parent $Fe_2(dobdc)$ MOF, like most other MOFs, features unsaturated open metal sites and results in selectivity towards olefins over paraffins. By allowing the Fe centers to form Fe–peroxo bonds on the pore surface, the MOF effectively switched the selectivity from ethylene to ethane. Further analysis from neutron powder diffraction demonstrated that deuterated ethane molecule (C_2D_6) was bonded through the peroxo-group by forming a relatively strong hydrogen bond. In addition, the size and shape of ethane molecules matches with the pore geometry thereby originating stronger van der Waals interactions between ethane and pore surface. These effects culminated in a selectivity of 4.4 for ethane compared to that of ethylene.

Although $Fe_2(O_2)(dobdc)$ MOF exhibits good selectivity and ethane uptake, the structure is not stable in air and also requires higher energy for regeneration. To overcome this issue, fabricating adsorbents that combine high selectivity with uptake is of special interest. A robust MOF termed MUF-15 was synthesized using inexpensive precursors such as cobalt acetate and isophthalic acid (H_2ipa) in a water/methanol mixture. The structure shows selective ethane uptake over ethylene with a selectivity of two and can be easily regenerated and recycled without any loss in the separation performance. MUF-15 represents a rare combination of MOF structure consisting of both high pore volume and pore size closing matching with the guest molecule that shows distinct preference for adsorbing ethane reaching almost 4.69 mmol/g at 293 K and 1 bar. In addition, 1 kg of this MOF produces nearly 14 L of ethylene in a single adsorption cycle based on an equimolar C_2H_4/C_2H_6 mixture. To delve deeper into the adsorption mechanism of selective ethane/ethylene adsorption in MUF-15, first principles dispersion-corrected DFT-D3 calculations were performed. The predicted static binding energy for ethane is around -36.7 kJ/mol, whereas it is 35.0 kJ/mol for ethylene, which is in accordance with the experimental values. As shown in Figures 7A and 7B, the preferred binding site identified from DFT calculation for ethane molecules is located in a pocket surrounded by four phenyl rings. The stronger host-guest interactions can be attributed to van der Waals interaction between the C_2H_6 and the neighboring π electron clouds. There exists $C-H \cdots \pi$ interactions between all six hydrogens of ethane and three adjacent phenyl rings, dominated by dispersion interaction, as compared to other noncovalent interactions involving permanent dipoles/quadrupoles.

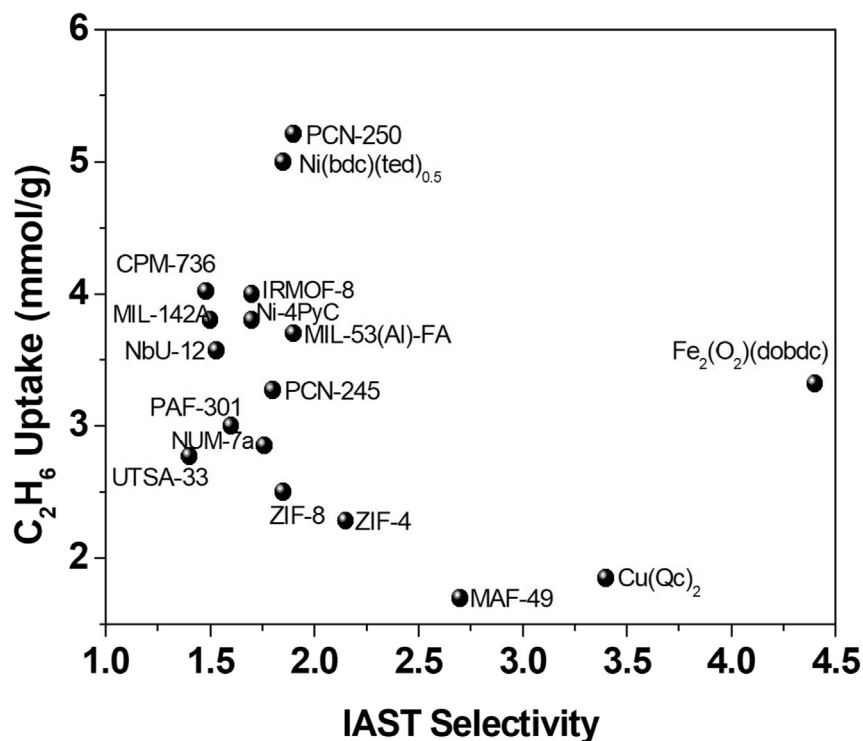


Figure 8. IAST selectivity for 1:1 (v/v) C₂H₆/C₂H₄ and C₂H₆ uptake for some of the best performing MOFs at 1 bar and room temperature

However, for ethylene molecule, its lower binding energy can be attributed to the reduce number of C-H... π interaction and to the lack of strong permanent dipoles on the framework. Besides dispersion interaction, C₂H₆ a more polarizable molecule can interact more strongly by the induced dipole interactions with the framework compared to the less polarizable C₂H₄ molecule. Overall, MUF-15 possesses good regenerability, stability and productivity, making it an ideal adsorbent material for selective separation of ethane over ethylene in industrial settings (Qazvini et al., 2019a, 2019b).

There exists a trade-off between adsorption selectivity and capacity in a separation process at industrial conditions, with high selectivity results in high degree of purity with less cycles needed, but with high capacity the regeneration time is longer. Figure 8 shows the IAST calculated C₂H₆/C₂H₄ selectivity and C₂H₆ uptake for several top performing MOFs at 298 K and 1 bar. Ultimately, for an adsorbent material to be used in industrial scale, several other factors such as cost, scale-up, stability and regenerability need to be considered. A different approach was undertaken by maximizing the larger number of intermolecular interactions between C₂H₆ and the host to make a MOF structure more selective to ethane over ethylene (Lin et al., 2018a, 2018b; Liao et al., 2015). To demonstrate this effect, authors synthesized two MOFs, Cu(ina)₂ (ina = isonicotinic acid) and Cu(Qc)₂ (Qc = quinoline5-carboxylic acid). These two isorecticular MOFs possess hydrophobic interiors with lack of strong adsorption sites that led authors to study ethane and ethylene separation. The Cu(ina)₂ MOF featured larger pores and was only slightly selective to ethane. The Cu(Qc)₂, however, possessed smaller pores and demonstrated the highest ethane selectivity of 3.4, which was achieved by maximizing the contact area between ethane molecule and the pore surface thereby allowing the better adsorbent-adsorbate interactions. The same group extended this concept by designing a hydrogen bonded framework known as HOF-76a by avoiding strong hydrogen bonding donors. The pore structure of HOF-76a shows a non-polar surface with triangular channels. These structures enable it to preferentially adsorb ethane over ethylene with a IAST selectivity of 2 at 296K and 1 bar pressure.

In addition to separation, the research has also been directed to develop a method to maximize the ethane uptake of a MOFs with an aim to achieve a high ethylene recovery from the outlet stream (Yang et al., 2020a,

2020b). In this study, a method was developed by using a pore-space-partition strategy in which a partitioning agent (organic ligand) was introduced into the hexagonal channels resulting in the partitioned *acs* net known as a *pacs* net. In addition, the partitioning agent helps in two ways. First, it eliminates the open metal site (OMS) that is responsible for preferential binding to ethylene molecule by π complexation. Eliminating the OMS allows the pore surfaces to be relatively inert and hence could support as an ideal adsorption site for ethane molecules. Second, partitioning of the pores creates an ideal geometry of the pore surface that can well fit the ethane molecule for its preferential adsorption. These effects culminated into the generation of several MOFs with remarkable ethane uptake capacity of as high as 154.2 cm³/g [compared to a ethane uptake is 74.3 cm³/g showed by Fe(O₂) (dobdc)] with a relatively lower selectivity of 1.75 for ethane compared to that of ethylene. Despite the lower selectivity, its high ethane uptake makes it competitive for the separation of ethane from ethylene with the added benefit of being more stable and requiring less energy for regeneration.

Although there is a lot of recent development in generating ethane selective MOFs (Tang and Jiang, 2020; Solanki and Borah, 2020) there has been rather a few developments in making propane selective MOFs. The most propane selective MOF to date is [Ni(bpe)₂(WO₄)] (bpe = 1,2-bis(4-pyridyl)ethylene) which was reported in 2020 (Yang et al., 2019). The Ni(bpe)₂(WO₄) MOF forms a catenated cage that has a cavity size of 5.6 Å, lined with aromatic groups. This cavity size is close to the kinetic diameter of propane. This typical size of the cage resembles a close fit of the propane molecule thereby allowing better van der Waals interactions between propane molecule and pore surface. The electronegative aromatic groups present on the pore surface also provided additional binding sites for propane adsorption. These effects allow the Ni(bpe)₂(WO₄) to display a propane selectivity in the range of 1.62–2.75. Despite this success, the uptakes and selectivity of propane selective MOFs are well behind those of ethane selective MOFs and more research on material development is required.

For carbonaceous adsorbents, the selectivity toward ethane is usually harnessed by the interactions between ethylene and polar heteroatom content of the carbon surface, like oxygen and nitrogen. The carbonaceous adsorbents were synthesized from the precursor of fructose (Xiao et al., 2018) for oxygen functionalized carbon and polydopamine (Liang et al., 2018) or glucosamine (Wang et al., 2019a, 2019b) for nitrogen-doped carbon. IAST-based selectivity of ethane over ethylene was reported to be as high as (Liang et al., 2018) 20 in the lowest pressure and ethane to ethylene ratio of 1:15. DFT calculations revealed that (Liang et al., 2018; Wang et al., 2019a, 2019b) pristine sp² hybridized carbon surface favors ethylene adsorption owing to the π - π interactions between ethylene and delocalized π bond of carbon. However, introduction of few oxygen and nitrogen functional groups on the carbon surface is proven to strongly favor the ethane molecule. The oxygen functional groups that were confirmed to favor ethane adsorption are hydroxyl, carboxylate and ketone groups, whereas the nitrogen-containing groups that demonstrated ethane selectivity are graphitic and pyridinic nitrogen. The calculations found that carboxylate group is the most effective in attracting ethane with the adsorption energy of -44.6 kJ/mol (for ethylene: -39.2 kJ/mol), whereas graphitic nitrogen is most effective among nitrogen functionalities with adsorption energy of ethane as -13.4 kJ/mol (for ethylene: -12 kJ/mol). A different computation study revealed that introduction of N or O functionalities on sp² hybridized carbon decreases the bond distance between carbon surface and ethane molecule from 3.34 Å to 3.03 Å, whereas such occurrence increases bond distance between carbon surface and ethylene from 3.30 Å to 3.68 Å, thereby favoring the ethane molecule. Besides calculation, a hypothesis was also put forward incorporating van der Waals's force as a contributing factor. It is claimed that enhanced van der Waals's force could be responsible for the enhanced adsorption of ethane compared to ethylene (Wang et al., 2019a, 2019b). It is postulated that a slightly larger size and high polarizability of ethane (kinetic diameter: 4.44 Å, polarizability: 44.7 × 10²⁵ cm³) compared to that of ethylene (kinetic diameter: 4.163 Å, polarizability: 42.5 × 10²⁵ cm³) are expected to cause a stronger van der Waal's force between ethane and carbon surface thereby increasing its adsorbed amount. Computation studies also revealed that ethane adsorption is better in the narrow micropores of 6–10 Å with the adsorption energy of ~6.6 kJ/mol compared to that of larger pores. Nonetheless, all the pores demonstrated the higher adsorption energy for ethane over ethylene.

It was also reported that nanoporous boron nitride (Saha et al., 2017) demonstrates selectivity of ethane and propane over ethylene and propylene, respectively, but the computational studies were not reported.

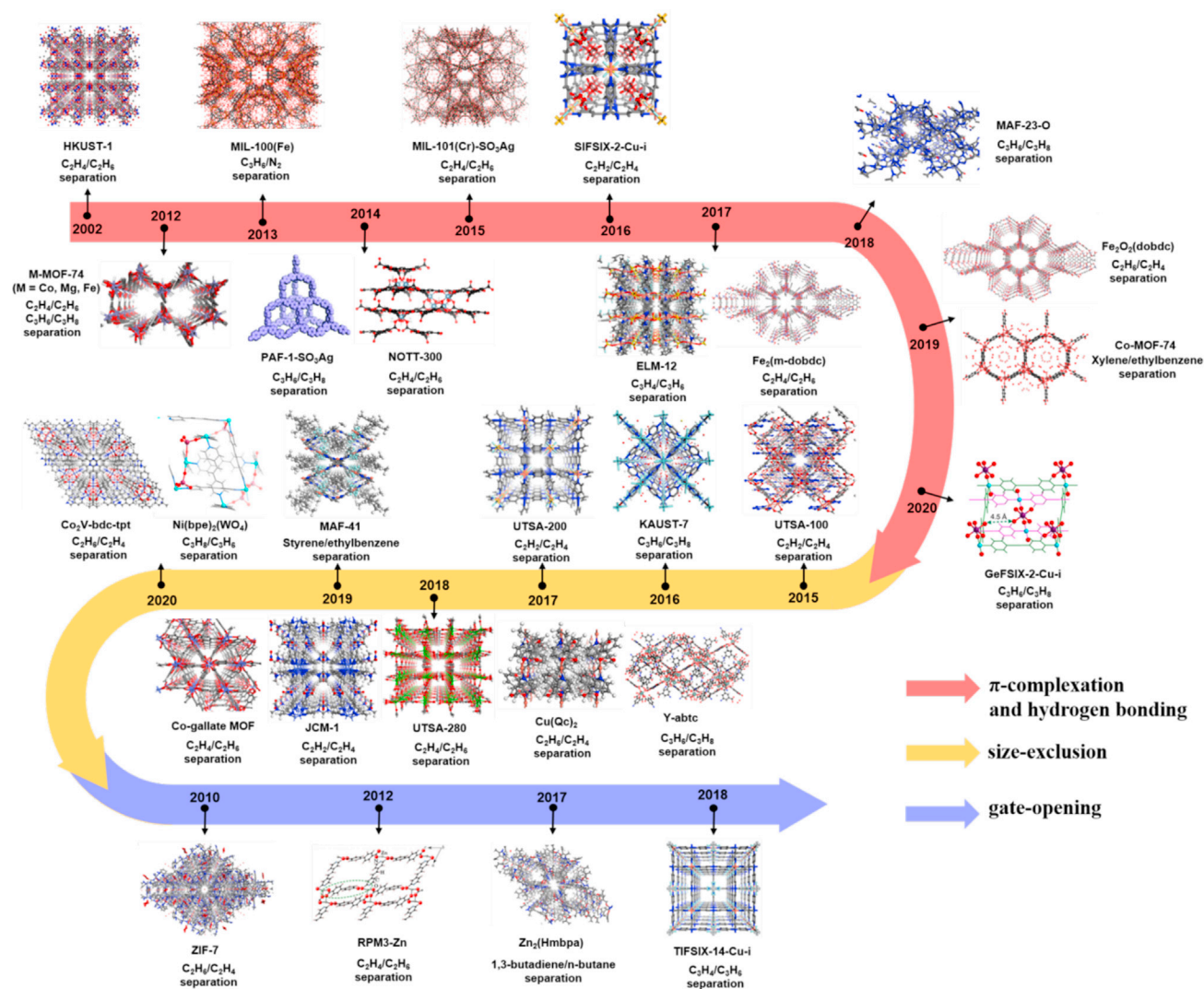


Figure 9. Different types of MOF-structures employed for olefin separation and their corresponding separation mechanisms

CONCLUSIONS AND FUTURE RECOMMENDATIONS

The study and research on the separation of light olefins and paraffins by adsorption have been very popular among researchers worldwide. There are several adsorbents that demonstrated remarkable paraffin-olefin separation performance. Among them, MOFs have proven to be a potential adsorbent for olefin and paraffin separation because of its large surface area and porosity, functionalized pore surface, and flexible pore size/shape. Starting with the first research on olefin and paraffin separation using MOF in 2002, MOFs have been developed to study olefin and paraffin separation until now. Considering the industrial demands of hydrocarbons, continuous research is needed in the future. In this paper, we have described several proposed separation mechanisms such as π -complexation, hydrogen bonding, kinetic separation, size-exclusion, and gate-opening of MOFs (Figure 9). As mentioned earlier, more research on paraffin-selective adsorbents should be explored in order to perform a low-energy intensive operation and to obtain high-purity olefins. The overall challenge of paraffin-olefin separation by adsorption arises from (a) materials perspective and (b) engineering perspective.

Despite some adsorbents, mostly MOFs have demonstrated unprecedented performance in paraffin-olefin separation, their real-world application could be limited by the high cost and energy input during synthesis phase as most of the synthesis protocol utilizes solvothermal technique. More research should be directed

towards alternative routes of synthesis, like mechanochemical or microwave methods. Recovery and recycling of spent solvent may also improve the cost of the synthesis as well.

Too properly understand the separation performance, column breakthrough experiments with the realistic conditions must be performed and it is quite encouraging to find that more and more scientific works with actual breakthrough experiments along with simulations are being reported. It is important to analyze the recovery and purity of the desired component as they do not always reciprocate with each other. It is also important to study the cyclability during the process of continuous adsorption and desorption. Enthalpy of adsorption and desorption during the cyclability is an important parameter to consider as heating of adsorption bed during loading and cooling of the same bed during desorption will influence the working capacity and operation cycle. In addition, most of the research works simulated the gas mixtures from the processing conditions of a conventional olefin source; however, with time, some other non-conventional techniques of generating light olefins are being popular, like oxidative coupling of methane (OCM), fluid catalytic cracking (FCC), and methanol to olefin (MTO) conversion. The future research work should also target the processing conditions of those olefin sources as well. Gas adsorption isotherms on mixture of gases constituting similar product mixture may also help understand the realistic separation condition as well.

It is recommended that more research, especially on the engineering side, needs to be performed to implement those adsorbents onto a large or industrial scale. Different factors that need to be examined are long-term stability, chemical resistance to surrounding environmental conditions, like moisture, regeneration and cyclability, pelletization, mechanical stability, good processability, cost of synthesizing/manufacturing of the adsorbents in large scale and overall economy of the PSA system. In the near future, all this information can be fed into a unified process simulation and optimization database that can be used to calculate the feasibility of using a particular adsorbent in designing a PSA system.

ACKNOWLEDGMENTS

This work was funded by American Chemical Society sponsored Petroleum Research Fund (ACS-PRF) with grant no. 59667-UR10. This work also was supported by the U.S. Department of Energy, Office of Science, Office of Basic Energy Sciences, Chemical Sciences, Geosciences, and Biosciences Division through its separation science program under award # DE-SC0021357. PKT and RB thank Dr. Daniel Matuszak and Dr Gopalsamy Karuppasamy for kind support. PNNL is a multiprogram national laboratory operated for the U.S. Department of Energy by Battelle Memorial Institute under Contract DE-AC05-76RL01830.

AUTHOR CONTRIBUTIONS

Conceptualization, Framework, Review and Editing, D.S.; Literature review, manuscript writing and Editing, D. S., M.B.K., A.R., R.B., P.K.T.; Funding acquisition and supervision, D.S.

DECLARATION OF INTERESTS

The authors declare no competing interests.

REFERENCES

- Anson, A., Wang, Y., Lin, C.C.H., Kuznicki, T.M., and Kuznicki, S.M. (2008). Adsorption of ethane and ethylene on modified ETS-10. *Chem. Eng. Sci.* *63*, 4171–4175.
- Bachman, J.E., Kapelewski, M.T., Reed, D.A., Gonzalez, M.I., and Long, J.R. (2017). M2(m-dobdc) (M = Mn, Fe, Co, Ni) metal-organic frameworks as highly selective, high-capacity adsorbents for olefin/paraffin separations. *J. Am. Chem. Soc.* *139*, 15363–15370.
- Bachman, J.E., Reed, D.A., Kapelewski, M.T., Chachra, G., Jonnavittula, D., Radaelli, G., and Long, J.R. (2018). Enabling alternative ethylene production through its selective adsorption in the metal-organic framework Mn2(m-dobdc). *Energy Environ. Sci.* *11*, 2423–2431.
- Bae, Y.S., Lee, C.Y., Kim, K.C., Farha, O.K., Nickias, P., Hupp, J.T., Nguyen, S.T., and Snurr, R.Q. (2012). High propene/propane selectivity in isostructural metal-organic frameworks with high densities of open metal sites. *Angew. Chem.* *124*, 1893–1896.
- Bao, Z., Wang, J., Zhang, Z., Xing, H., Yang, Q., Yang, Y., Wu, H., Krishna, R., Zhou, W., and Chen, B. (2018). Molecular sieving of ethane from ethylene through the molecular cross-section size differentiation in Gallate-based metal-organic frameworks. *Angew. Chem.* *57*, 16020–16025.
- Basaldella, E.I., Tara, J.C., Armenta, G.A., Patino-Iglesias, M.E., and Castell'on, E.R. (2006). Propane/propylene separation by selective olefin adsorption on Cu/SBA-15 mesoporous silica. *J. Sol-gel Sci. Technol.* *37*, 141–146.
- Bloch, E.D., Queen, W.L., Krishna, R., Zadrozny, J.M., Brown, C.M., and Long, J.R. (2012). Hydrocarbon separations in a metal-organic framework with open iron(II) coordination sites. *Science* *335*, 1606–1610.
- Cadiou, A., Adil, K., Bhatt, P.M., Belmabkhout, Y., and Eddaoudi, M. (2016). A metal-organic framework-based splitter for separating propylene from propane. *Science* *353*, 137–140.
- Chen, K.-J., Madden, D.G., Mukherjee, S., Pham, T., Forrest, K.A., Kumar, A., Space, B., Kong, J., Zhang, Q.-Y., and Zaworotko, M.J. (2019). Synergistic sorbent separation for one-step ethylene purification from a four-component mixture. *Science* *366*, 241–246.

- Chen, C.X., Wei, Z.-W., Pham, T., Lan, P.C., Forest, K.A., Chrn, S., El-Enizi, A.M., Nafady, A., Su, C.Y., and Ma, S. (2021). Nanospace engineering of metal-organic frameworks through dynamic spacer installation of multifunctionalities for efficient separation of ethane from ethane/ethylene mixtures. *Angew. Chem.* **60**, 9680–9685.
- Cui, X., Chen, K., Xing, H., Yang, Q., Krishna, R., Bao, Z., Wu, H., Zhou, W., Dong, X., Han, Y., et al. (2016). Pore chemistry and size control in hybrid porous materials for acetylene capture from ethylene. *Science* **353**, 141–144.
- Van Den Bergh, J., Gücüyener, C., Pidko, E.A., Hensen, E.J., Gascon, J., and Kapteijn, F. (2011). Understanding the anomalous alkane selectivity of ZIF-7 in the separation of light alkane/alkene mixtures. *Chem. Eur. J.* **17**, 8832–8840.
- Desiraju, G.R. (2002). Hydrogen bridges in crystal engineering: interactions without borders. *Acc. Chem. Res.* **35**, 565–573.
- Dey, A., Maity, B., Bhatt, P.M., Ghosh, M., Cavallo, L., Eddoudi, M., and Khashab, N.M. (2021). Adsorptive molecular sieving of styrene over ethylbenzene by trianglimine crystals. *J. Am. Chem. Soc.* **143**, 4090–4094.
- Do, D.D. (1998). *Adsorption Analysis: Equilibria and Kinetics* (Imperial College Press). <https://doi.org/10.1142/p111>.
- Gao, F., Wang, Y., Wang, X., and Wang, S. (2016). Ethylene/ethane separation by CuCl/AC adsorbent prepared using CuCl₂ as a precursor. *Adsorption* **22**, 1013–1022.
- Gehre, M., Guo, Z., Rothenberg, G., and Tanase, S. (2017). Sustainable separations of C₄-hydrocarbons by using microporous materials. *ChemSusChem* **10**, 3947–3963.
- Gonzalez, M.I., Kapelewski, M.T., Bloch, E.D., Milner, P.J., Reed, D.A., Hudson, M.R., Mason, J.A., Barin, G., Brown, C.M., and Long, J.R. (2018). Separation of xylene isomers through multiple metal site interactions in metal-organic frameworks. *J. Am. Chem. Soc.* **140**, 3412–3422.
- Grande, C.A., Araujo, J.D.P., Cavenati, S., Firpo, N., Basaldella, E., and Rodrigues, A.E. (2004). New π -complexation adsorbents for propane-propylene separation. *Langmuir* **20**, 5291–5297.
- Grande, C.A., Gascon, J., Kapteijn, F., and Rodrigues, A.E. (2010). Propane/propylene separation with Li-exchanged zeolite 13X. *Chem. Eng. J.* **160**, 207–214.
- Gutiérrez-Sevillano, J.J., Dubbeldam, D., Rey, F., Valencia, S., Palomino, M., Martín-Calvo, A., and Calero, S. (2010). Analysis of the ITQ-12 zeolite performance in propane-propylene separations using a combination of experiments and molecular simulations. *J. Phys. Chem. C* **114**, 14907–14914.
- Gücüyener, C., Van Den Bergh, J., Gascon, J., and Kapteijn, F. (2010). Ethane/ethene separation turned on its head: selective ethane adsorption on the metal-organic framework ZIF-7 through a gate-opening mechanism. *J. Am. Chem. Soc.* **132**, 17704–17706.
- Han, S.-S., Park, J.-H., Kim, J.-N., and Cho, S.-H. (2005). Propylene recovery from propylene/propane/nitrogen mixture by PSA process. *Adsorption* **11**, 621–624.
- Hedin, N., DeMartin, G.J., Roth, W.J., Strohmaier, K.G., and Reyes, S.C. (2008). PFG NMR self-diffusion of small hydrocarbons in high silica DDR, CHA and LTA structures. *Microporous Mesoporous Mater.* **109**, 327–334.
- Hu, T.-L., Wang, H., Li, B., Krishna, R., Wu, H., Zhou, W., Zhao, Y., Han, Y., Wang, X., Zhu, W., et al. (2015). Microporous metal-organic framework with dual functionalities for highly efficient removal of acetylene from ethylene/acetylene mixtures. *Nat. Commun.* **6**, 7328.
- Iucolano, F., Aprea, P., Caputo, D., Colella, C., Eic, M., and Huang, Q. (2008). Adsorption and diffusion of propane and propylene in Ag⁺-impregnated MCM-41. *Adsorption* **14**, 241–246.
- Jiang, D., Sumpter, B.G., and Dai, S. (2006). Olefin adsorption on silica-supported silver salts: a DFT study. *Langmuir* **22**, 5716–5722.
- Jiang, W.-J., Sun, L.-B., Yin, Y., Song, X.-L., and Liu, X.-Q. (2013). Ordered mesoporous carbon CMK-3 modified with Cu(I) for selective ethylene/ethane adsorption. *Sep. Sci. Technol.* **48**, 968–976.
- Kargol, M., Zajac, J., Jones, D.J., Steriotis, T., Rozie'ra, J., and Vitse, P. (2004). Porous silica materials derivatized with Cu and Ag cations for selective propene-propane adsorption from the gas phase: aluminosilicate ion-exchanged monoliths. *Chem. Mater.* **16**, 3911–3918.
- Lamia, N., Jorge, M., Granato, M.A., Paz, F.A.A., Chevreau, H., and Rodrigues, A.E. (2009). Adsorption of propane, propylene and isobutane on a metal-organic framework: molecular simulation and experiment. *Chem. Eng. Sci.* **64**, 3246–3259.
- Lee, C.Y., Bae, Y.-S., Jeong, N.C., Farha, O.K., Sarjeant, A.A., Stern, C.L., Nickias, P., Snurr, R.Q., Hupp, J.T., and Nguyen, S.T. (2011). Kinetic separation of propene and propane in metal-organic frameworks: controlling diffusion rates in plate-shaped crystals via tuning of pore apertures and crystallite aspect ratios. *J. Am. Chem. Soc.* **133**, 5228–5231.
- Li, K., Olson, D.H., Seidel, J., Emge, T.J., Gong, H., Zeng, H., and Li, J. (2009). Zeolitic imidazolate frameworks for kinetic separation of propane and propene. *J. Am. Chem. Soc.* **131**, 10368–10369.
- Li, B., Zhang, Y., Krishna, R., Yao, K., Han, Y., Wu, Z., Ma, D., Shi, Z., Pham, T., Space, B., et al. (2014). Introduction of π -complexation into porous aromatic framework for highly selective adsorption of ethylene over ethane. *J. Am. Chem. Soc.* **136**, 8654–8660.
- Li, B.B., Cui, X., O'Nolan, D., Wen, H.-M., Jiang, M., Krishna, R., Wu, H., Lin, R.-B., Chen, Y.-S., Yuan, D., et al. (2017a). An ideal molecular sieve for acetylene removal from ethylene with record selectivity and productivity. *Adv. Mater.* **29**, 1704210.
- Li, L., Lin, R.-B., Krishna, R., Wang, X., Li, B., Wu, H., Li, J., Zhou, W., and Chen, B. (2017b). Flexible-robust metal-organic framework for efficient removal of propyne from propylene. *J. Am. Chem. Soc.* **139**, 7733–7736.
- Li, L., Lin, R.-B., Krishna, R., Li, H., Xiang, S., Wu, H., Li, J., Zhou, W., and Chen, B. (2018). Ethane/ethylene separation in a metal-organic framework with iron-peroxo sites. *Science* **362**, 443–446.
- Liang, W., Wu, Y., Xiao, H., Xiao, J., Li, Y., and Li, Z. (2018). Ethane-selective carbon composites CPDA@A-ACs with high uptake and its enhanced ethane/ethylene adsorption selectivity. *Aiche J.* **64**, 3390–3399.
- Liang, B., Zhang, X., Xie, Y., Lin, R.-B., Krishna, R., Cui, H., Li, Z., Shi, Y., Wu, H., and Zhou, W. (2020). An ultramicroporous metal-organic framework for high sieving separation of propylene from propane. *J. Am. Chem. Soc.* **142**, 17795–17801.
- Liao, P.-Q., Zhang, W.-X., Zhang, J.-P., and Chen, X.-M. (2015). Efficient purification of ethene by an ethane-trapping metal-organic framework. *Nat. Commun.* **6**, 8697.
- Liao, P.-Q., Huang, N.-Y., Zhang, W.-X., Jhang, J.-P., and Chen, X.-M. (2017). Controlling guest conformation for efficient purification of butadiene. *Science* **356**, 1193–1196.
- Lin, R.-B., Li, L., Zhou, H.-L., Wu, H., He, C., Li, S., Krishna, R., Li, J., Zhou, W., and Chen, B. (2018a). Molecular sieving of ethylene from ethane using a rigid metal-organic framework. *Nat. Mater.* **17**, 1128–1133.
- Lin, R.-B., Wu, H., Li, L., Tang, X.-L., Li, Z., Gao, J., Cui, H., Zhou, W., and Chen, B. (2018b). Boosting ethane/ethylene separation within isorecticular ultramicroporous metal-organic frameworks. *J. Am. Chem. Soc.* **140**, 12940–12946.
- Lin, R.-B., He, Y., Li, P., Wang, H., Zhou, W., and Chen, B. (2019). Multifunctional porous hydrogen-bonded organic framework materials. *Chem. Soc. Rev.* **48**, 1362–1389.
- Liu, J., Liu, Y., Talay, D.K., Calverley, E., Brayden, M., and Martinez, M. (2015). A new carbon molecular sieve for propylene/propane separations. *Carbon* **85**, 201–211.
- Liu, J., Calverley, E.M., McAdon, M.H., Goss, J.M., Liu, Y., Andrews, K.C., Wolford, T.D., Beyer, D.E., Han, C.S., Anaya, D.A., et al. (2017). New carbon molecular sieves for propylene/propane separation with high working capacity and separation factor. *Carbon* **123**, 273–282.
- De Luca, G.D., Saha, D., and Chakraborty, S. (2021). Why Ag(I) grafted porous carbon matrix prefers alkene over alkane? An inside view from ab-initio study. *Microporous Mesoporous Mater.* **316**, 110940.
- Luna-Triguero, A., Sławek, A., Sánchez-de-Armas, R., Gutiérrez-Sevillano, J.J., Ania, C.O., Parra, J.B., Vicent-Luna, J.M., and Calero, S. (2020). π -Complexation for olefin/paraffin separation using aluminosilicates. *Chem. Eng. J.* **380**, 122482.
- Lyndon, R., You, W., Ma, Y., Bacsa, J., Gong, Y., Stangland, E.E., Walton, K.S., Sholl, D.S., and Lively, R.P. (2020). Tuning the structures of metal-organic frameworks via a mixed-linker strategy for ethylene/ethane kinetic separation. *Chem. Mater.* **32**, 3715–3722.
- Miltenburg, A.V., Zhu, W., Kapteijn, F., and Moulijn, J.A. (2006). Adsorptive separation of light olefin/paraffin mixtures. *Chem. Eng. Res. Des.* **84**, 350–354.

- Molero, H., Bartlett, B.F., and Tysoe, W.T. (1999). The hydrogenation of acetylene catalyzed by palladium: hydrogen pressure dependence. *J. Catal.* **181**, 49–56.
- Moulijn, J.A., Makkee, M., and van Diepen, A. (2001). *Chemical Process Technology* (John Wiley & Sons). <https://doi.org/10.1002/aoc.202>.
- Myers, A.L., and Prausnitz, J.M. (1965). Thermodynamics of mixed-gas adsorption. *Aiche J.* **11**, 121–127.
- Nijem, N., Wu, H., Canepa, P., Marti, A., Balkus, K.J., Jr., Thonhauser, T., Li, J., and Chabal, Y.J. (2012). Tuning the gate opening pressure of metal–organic frameworks (MOFs) for the selective separation of hydrocarbons. *J. Am. Chem. Soc.* **134**, 15201–15204.
- Palomino, M., Cantin, A., Corma, A., Leiva, S., Rey, F., and Valencia, S. (2007). Pure silica ITQ-32 zeolite allows separation of linear olefins from paraffins. *Chem. Commun.* **2007**, p1233–1235.
- Pu, S., Wang, J., Li, L., Zhang, Z., Bao, Z., Yang, Q., Yang, Y., Xing, H., and Ren, Q. (2018). Performance comparison of metal–organic framework extrudates and commercial zeolite for ethylene/ethane separation. *Ind. Eng. Chem. Res.* **57**, 1645–1654.
- Qazvini, O.T., Babarao, R., and Telfer, S.G. (2019a). Multipurpose metal–organic framework for the adsorption of acetylene: ethylene purification and carbon dioxide removal. *Chem. Mater.* **31**, 4919–4926.
- Qazvini, O.T., Babarao, R., Shi, Z.-L., Zhang, Y.-B., and Telfer, S.G. (2019b). A robust ethane-trapping metal–organic framework with a high capacity for ethylene purification. *J. Am. Chem. Soc.* **141**, 5014–5020.
- Rege, S.U., Padin, J., and Yang, R.T. (1998). Olefin/paraffin separations by adsorption: π -complexation vs. kinetic separation. *Aiche J.* **44**, 799–809.
- Ribeiro, A.M., Campo, M.C., Narin, G., Santos, J.C., Ferreira, A., Chang, J.-S., Hwang, Y.K., Seo, Y.-K., Lee, U.-H., and Loureiro, J.M. (2013). Pressure swing adsorption process for the separation of nitrogen and propylene with a MOF adsorbent MIL-100(Fe). *Sep. Purif. Technol.* **110**, 101–111.
- Ruthven, D.M. (1984). *Principles of Adsorption and Adsorption Processes*, 1st edition (Wiley-Interscience), ISBN-13: 978-0471866060.
- Saha, D., and Deng, S. (2010). Characteristics of ammonia adsorption on activated alumina. *J. Chem. Eng. Data* **55**, 5587–5593.
- Saha, D., and Grappe, H.A. (2017). Adsorption properties of activated carbon fibers. In *Activated Carbon Fiber and Textiles*, J.Y. Chen, ed. (Elsevier), pp. 143–165. [10.1016/B978-0-08-100660-3.00005-5](https://doi.org/10.1016/B978-0-08-100660-3.00005-5).
- Saha, D., Wei, Z., and Deng, S. (2008). Equilibrium, kinetics and enthalpy of hydrogen adsorption in MOF-177. *Int. J. Hydrogen Energy* **33**, 7479–7488.
- Saha, D., Bao, Z., Jia, F., and Deng, S. (2010). Adsorption of CO₂, CH₄, N₂O, and N₂ on MOF-5, MOF-177, and zeolite 5A. *Environ. Sci. Technol.* **44**, 1820–1826.
- Saha, D., Grappe, H., Chakraborty, A., and Orkoulas, G. (2016). Post extraction separation, on-board storage and catalytic conversion of methane in natural gas: a review. *Chem. Rev.* **116**, 11436–11499.
- Saha, D., Orkoulas, G., Yohannan, S., Ho, H.-C., Cakmak, E.J., Chen, S., and Ozcan, S. (2017). Nanoporous boron nitride as exceptionally thermally stable adsorbent: role in efficient separation of light hydrocarbons. *ACS Appl. Mater. Interfaces* **9**, 14506–14517.
- Saha, D., Toof, B., Krishna, R., Orkoulas, G., Gismondini, P., Thorpe, R., and Comroe, M. (2020). Separation of ethane-ethylene and propane-propylene by Ag(I) doped and sulfurized microporous carbon. *Microporous Mesoporous Mater.* **299**, 110099–110101.
- Schmittmann, S., Pasel, C., Luckas, M., and Bathen, D. (2020). Adsorption of light alkanes and alkenes on activated carbon and zeolite 13x at low temperatures. *J. Chem. Eng. Data* **65**, 706–716.
- Schulze, J., and Homann, M. (1989). *Processes of Separation and Transformation in C4-Chemistry, C4-Hydrocarbons and Derivatives*, © Springer-Verlag Berlin Heidelberg, pp. 35-106, Online ISBN 978-3-642-73858-6. https://doi.org/10.1007/978-3-642-73858-6_4.
- Selzer, C., Werner, A., and Kaskel, S. (2018). Selective adsorption of propene over propane on hierarchical zeolite ZSM-58. *Ind. Eng. Chem. Res.* **57**, 6609–6617.
- Sholl, D.S., and Lively, R.P. (2016). Seven chemical separations to change the world. *Nat. News* **532**, 435–437.
- Solanki, V.A., and Borah, B. (2020). In-silico identification of adsorbent for separation of ethane/ethylene mixture. *J. Mol. Model* **26**, 353–368.
- Tang, H., and Jiang, J. (2020). In silico screening and design strategies of ethane-selective metal–organic frameworks for ethane/ethylene separation. *Aiche J.* **67**, e17025.
- Tan, Q., Peng, Y., Xue, W., Huang, H., Liu, D., and Zhong, C. (2019). Ultramicroporous metal–organic framework with polar groups for efficiently recovering propylene from polypropylene off-gas. *Ind. Eng. Chem. Res.* **58**, 14333–14339.
- Torres-Knoop, A., Heinen, J., Krishna, R., and Dubbeldam, D. (2015). Entropic separation of styrene/ethylbenzene mixtures by exploitation of subtle differences in molecular configurations in ordered crystalline nanoporous adsorbents. *Langmuir* **31**, 3771–3778.
- Wang, H., Dong, X., Colombo, V., Wang, Q., Liu, Y., Liu, W., Wang, X.L., Huang, X.Y., Proserpio, D.M., and Sironi, A. (2018a). Tailor-made microporous metal–organic frameworks for the full separation of propane from propylene through selective size exclusion. *Adv. Mater.* **30**, 1805088.
- Wang, H., Dong, X., Lin, J., Teat, S.J., Jensen, S., Cure, J., Alexandrov, E.V., Xia, Q., Tan, K., Wang, Q., Olson, D.H., et al. (2018b). Topologically guided tuning of Zr-MOF pore structures for highly selective separation of C₆ alkane isomers. *Nat. Commun.* **9**, 1745.
- Wang, X., Wu, Y., Peng, J., Wu, Y., Xiao, X., Xia, Q., and Li, Z. (2019a). Novel glucosamine-based carbon adsorbents with high capacity and its enhanced mechanism of preferential adsorption of C₂H₆ over C₂H₄. *Chem. Eng. J.* **358**, 1114–1125.
- Wang, Y., Huang, N.Y., Zhang, X.W., He, H., Huang, R.K., Ye, Z.M., Li, Y., Zhou, D.D., Liao, P.Q., and Chen, X.M. (2019b). Selective aerobic oxidation of a metal–organic framework boosts thermodynamic and kinetic propylene/propane selectivity. *Angew. Chem.* **131**, 7774–7778.
- Wang, X., Zhang, P., Zhang, Z., Yang, L., Ding, Q., Cui, X., Wang, J., and Xing, H. (2020). Efficient separation of propene and propane using anion-pillared metal–organic frameworks. *Ind. Eng. Chem. Res.* **59**, 3531–3537.
- Xiao, H., Wu, Y., Wang, X., Peng, J., Xia, Q., and Li, Z. (2018). A novel fructose-based adsorbent with high capacity and its ethane-selective adsorption property. *J. Solid State Chem.* **268**, 190–197.
- Yang, R.T. (1987). *Gas Separation Adsorption Processes* (Imperial College Press), ISBN 10 1860940471.
- Yang, S., Ramirez-Cuesta, A.J., Newby, R., Garcia-Sakai, V., Manuel, P., Callear, S.K., Campbell, S.I., Tang, C.C., and Schroder, M. (2015). Supramolecular binding and separation of hydrocarbons within a functionalized porous metal–organic framework. *Nat. Chem.* **7**, 121–129.
- Yang, L., Cui, X., Yang, Q., Qian, S., Wu, H., Bao, Z., Zhang, Z., Ren, Q., Zhou, W., Chen, B., and Xing, H. (2018a). A single-molecule propyne trap: highly efficient removal of propyne from propylene with anion-pillared ultramicroporous materials. *Adv. Mater.* **30**, 1705374.
- Yang, L., Cui, X., Zhang, Y., Yang, Q., and Xing, H. (2018b). A highly sensitive flexible metal–organic framework sets a new benchmark for separating propyne from propylene. *J. Mater. Chem. A* **6**, 24452–24458.
- Yang, H., Wang, Y., Krishna, R., Jia, X., Wang, Y., Hong, A.N., Dang, C., Castillo, H.E., Bu, X., and Feng, P. (2020a). Pore-space-partition-enabled exceptional ethane uptake and ethane-selective ethane–ethylene separation. *J. Am. Chem. Soc.* **142**, 2222–2227.
- Yang, L., Cui, X., Ding, Q., Wang, Q., Jin, A., Ge, L., and Xing, H. (2020b). Polycatenated molecular cage-based propane trap for propylene purification with recorded selectivity. *ACS Appl. Mater. Interfaces* **12**, 2525–2530.
- Ye, Z.-M., He, C.-T., Xu, Y.-T., Krishna, R., Xie, Y., Zhou, D.-D., Zhou, H.-L., Zhang, J.-P., and Chen, X.-M. (2017). A new isomeric porous coordination framework showing single-crystal to single-crystal structural transformation and preferential adsorption of 1,3-butadiene from C₄ hydrocarbons. *Cryst. Growth Des.* **17**, 2166–2171.

Yoon, J.W., Seo, Y.K., Hwang, Y.K., Chang, J.S., Leclerc, H., Wuttke, S., Bazin, P., Vimont, A., Daturi, M., and Bloch, E. (2010). Controlled reducibility of a metal–organic framework with coordinatively unsaturated sites for preferential gas sorption. *Angew. Chem.* *49*, 5949–5952.

Zhang, Y., Li, B., Krishna, R., Wu, Z., Ma, D., Shi, Z., Pham, T., Forrest, K., Space, B., and Ma, S. (2015). Highly selective adsorption of ethylene over ethane in a MOF featuring the combination of open metal site and π -complexation. *Chem. Comm.* *51*, 2714–2717.

Zhang, Z., Peh, S.B., Wang, Y., Kang, C., Fan, W., and Zhao, D. (2020). Efficient trapping of trace acetylene from ethylene in an ultramicroporous metal–organic framework: synergistic effect of high-density open metal and electronegative sites. *Angew. Chem. Int. Ed.* *59*, 18927–18932.

Zhang, X., Cui, H., Lin, R.-B., Krishna, R., Zhang, Z.-Y., Liu, T., Liang, B., and Chen, B. (2021). Realization of ethylene production from its quaternary mixture through metal–organic framework materials. *ACS Appl. Mater. Interfaces* *13*, 22514–22520.

Zhou, D.-D., Chen, P., Wang, C., Wang, S.-S., Du, Y., Yan, H., Ye, Z.-M., He, C.-T., Huang, R.-K., and Mo, Z.-W. (2019). Intermediate-sized molecular sieving of styrene from larger and smaller analogues. *Nat. Mater.* *18*, 994–998.

Zhu, B., Mukherjee, S., Pham, T., Zhang, T., Wang, T., Jiang, X., Forrest, K.A., Zaworotko, M.J., and Chen, K.-J. (2021). Pore engineering for one-step ethylene purification from a three-component hydrocarbon mixture. *J. Am. Chem. Soc.* *143*, 1485–1492.